CENTRAL RESEARCH LIBRARY
ORNL-TM-4331
cy. 66

OAK RIDGE NATIONAL LABORATORY LIBRARIES
3 4456 0550195 3

LMFBR SAFETY AND CORE SYSTEMS PROGRAMS PROGRESS REPORT FOR MAY—JUNE 1973

M. H. Fontana

[redacted]

OAK RIDGE NATIONAL LABORATORY
CENTRAL RESEARCH LIBRARY
DOCUMENT COLLECTION
LIBRARY LOAN COPY
DO NOT TRANSFER TO ANOTHER PERSON
If you wish someone else to see this document, send in name with document and the library will arrange a loan.
UCN-7969
(3 3-67)

OAK RIDGE NATIONAL LABORATORY
OPERATED BY UNION CARBIDE CORPORATION • FOR THE U.S. ATOMIC ENERGY COMMISSION

Printed in the United States of America. Available from
the U.S. Atomic Energy Commission, Technical Information Center
P.O. Box 62, Oak Ridge, Tennessee 37830
Price: Printed Copy $5.45 ; Microfiche $0.95

This report was prepared as an account of work sponsored by the United States Government. Neither the United States nor the United States Atomic Energy Commission, nor any of their employees, nor any of their contractors, subcontractors, or their employees, makes any warranty, express or implied, or assumes any legal liability or responsibility for the accuracy, completeness or usefulness of any information, apparatus, product or process disclosed, or represents that its use would not infringe privately owned rights.

ORNL-TM-4331
UC-79e, UC-79p

Contract No. W-7405-eng-26

LMFBR SAFETY AND CORE SYSTEMS PROGRAMS PROGRESS REPORT FOR MAY–JUNE 1973

M. H. Fontana

OCTOBER 1973

NOTICE: This document contains information of a preliminary nature and was prepared primarily for internal use at the Oak Ridge National Laboratory. It is subject to revision or correction and therefore does not represent a final report.

OAK RIDGE NATIONAL LABORATORY
Oak Ridge, Tennessee 37830
operated by
UNION CARBIDE CORPORATION
for the
U.S. ATOMIC ENERGY COMMISSION

OAK RIDGE NATIONAL LABORATORY LIBRARIES

3 4456 0550195 3

CONTENTS

	Page
PREVIOUS LMFBR PROGRESS REPORTS	v
SUMMARY	vii
1. PROGRAM COORDINATION	1
2. ANALYSIS AND DATA EVALUATION	2
Results of Bundle 3A Experiments	2
Test Section Arrangement	2
Rod bundle instrumentation	3
Experiments Performed	5
Results	6
Temperatures in the central subchannels	6
Exit temperatures	17
Normalized temperatures of heater internal thermocouples	21
Normalized temperatures of wire-wrap and exit thermocouples	22
Conclusions	22
Effect of Six-Channel Internal Blockage in a Full-Size Fuel Subassembly	23
Status of ØRRIBLE Code Versions	26
3. WATER SYSTEM MOCKUP OF THE FFM FACILITY	29
4. FFM DYNAMIC TESTING AND NOISE ANALYSIS	38
5. FFM FACILITY ACTIVITIES	40
Test Bundle Operation	40
Bundle 1B	40
Test series IV (bundle 3A) test operation	41
Status of Design and Construction of Test Bundles	44
Bundle 5A	44
Test program	56
Special tests	57
Bundle 4A	58
Flow Impedance Test	60
General	60
Anomalous behavior in auxiliary circuits	63
Flow impedance	65
Conclusions	65
6. HEATER DEVELOPMENT	67
Revision of AEC-RDT Standard P4-1	67
Heaters for the ANL OPERA Flow Blockage Test	67
Westinghouse-ARD Blanket Heaters	67
Review of HEDL Specification HWS-9178	68
PWR Fuel Pin Simulators for the ORNL BDHT Test	68

FFM Heaters 69
Heaters for FFM bundle 5A 69
Heaters for FFM bundle 4A 71
Advanced Heater Development 71
Category II heaters 71
Category II heaters with Kanthal A-1 heater elements 71
Qualifying manufacturers of category II heaters 75
Category III heaters 75
Evaluation of heater fabrication methods 75
Redesign of the heater test facility 76

PREVIOUS LMFBR PROGRESS REPORTS

Prior information on these projects was presented in the following:

ORNL Nuclear Safety Research and Development Program Bimonthly Reports

Period Covered	Report No.
September–October 1968	ORNL-TM-2425
November–December 1968	ORNL-TM-2479
January–February 1969	ORNL-TM-2533
March–April 1969	ORNL-TM-2588
May–June 1969	ORNL-TM-2663
July-August 1969	ORNL-TM-2718
September–October 1969	ORNL-TM-2777
November–December 1969	ORNL-TM-2829
January–February 1970	ORNL-TM-2919
March–April 1970	ORNL-TM-2984
May–June 1970	ORNL-TM-3061
July–August 1970	ORNL-TM-3122
September–October 1970	ORNL-TM-3212
November–December 1970	ORNL-TM-3263
January–February 1971	ORNL-TM-3342
March–April 1971	ORNL-TM-3411
May–June 1971	ORNL-TM-3483
July–August 1971	ORNL-TM-3554
September–October 1971	ORNL-TM-3623
November–December 1971	ORNL-TM-3670
January–February 1972	ORNL-TM-3738
March–April 1972	ORNL-TM-3831
May–June 1972	ORNL-TM-3900
July–August 1972	ORNL-TM-3973

LMFBR Safety and Core Systems Programs Progress Reports

Period Covered	Report No.
September–October 1972	ORNL-TM-4075
November–December 1972	ORNL-TM-4088
January–February 1973	ORNL-TM-4148
March–April 1973	ORNL-TM-4261

SUMMARY

1. Program Coordination

During this reporting period coordination has been maintained with HEDL, ANL, WARD, and RRD. A test was operated in cooperation with HEDL to observe whether an increase in flow impedance occurred during isothermal operation at 1100°F as was observed in CCTL and JOYO. A first draft of a FFTF backup document, The Effect of Partial Blockages in Simulated LMFBR Fuel Assemblies, was sent to RRD, HEDL, and WARD.

2. Analysis and Data Evaluation

Experiments performed with FFM bundle 3A (which has a six-channel internal blockage) were evaluated. Internal temperatures were less than 200°F higher than the sodium temperature would have been without the blockage, even at 60% flow and 10 kW/ft (which is higher than FFTF average power). The ØRRIBLE code seemed to predict quite well temperatures downstream of the recirculating zone behind the blockage. Indications are that a nonheat-generating blockage of the magnitude as that tested would not cause excessive temperatures in the rod bundle.

3. Water System Mockup of the FFM Facility

Heat transfer experiments were continued with the ANL FEFP P1 edge-channel-type blockage and half-size edge-row wire-wrap spacers. Circumferential variations in heat transfer coefficient around a corner rod with and without blockage were measured, as were variations with axial distance from the blockage. At the higher Reynolds numbers (9.40×10^4), the recovery in the heat transfer coefficient downstream from the blockage coincides strikingly with the visual observation of the length of the flow recirculation zone. Experiments were started in which salt is injected into the flow recirculation zone to measure the residence time of the fluid within it. Preliminary results indicate that the value of $\tau U/d$ is between 35 and 45, where τ is the mean life of the salt tracer, U is the velocity, and d is twice the largest dimension of the blockage plate normal to the wall.

4. FFM Dynamic Testing and Noise Analysis

Bundle 3A outlet rake thermocouple noise signals were recorded in analog form on magnetic tape to allow off-line analysis using a digital frequency analysis program on the hybrid computer. Preliminary analyses indicate that there are sufficient sodium temperature fluctuations at the rake thermocouple to provide signals at least an order of magnitude higher than the electrical interference noise introduced by the signal conditioning amplifier and tape recorder.

5. FFM Facility Activities

The bundle 3A testing program was continued. Test 4, with only the central seven rods heated, was run to determine mixing effects, and test 5, with three edge heaters operating simultaneously, was run to determine the extent of flow spiraling that occurs in the simulated infinite array of this bundle. Test 6, the approach-to-boiling experiment, has been redefined, and the feasibility is being investigated by using an attemperator to allow boiling temperatures in the bundle without exceeding 1300°F in the permanent loop piping. Bundle 5A (ANL FEFP P1 lead test) has been designed and built, and a test plan was revised on the basis of comments received on the preliminary test plan.

6. Heater Development

Revision 1 of AEC-RDT Standard P4-1T, Electric Heaters — Simulated LMFBR Fuel Pins, was completed and issued for approval. Assistance was given to the ANL OPERA program, to the Westinghouse-ARD blanket program, and to HEDL for their HTR-400 heater assembly for the Prototype Closed Loop Development Installation. Experience obtained in the work on LMFBR fuel pin simulators is being utilized to assist the PWR Blowdown Heat Transfer Separate Effects Program at ORNL. It was discovered that annealing of small Alumel thermal element wires which are internal to the heaters after cold work caused excessive grain growth that leads to brittle behavior. Development of category II and category III heaters is continuing.

1. PROGRAM COORDINATION

M. H. Fontana R. E. MacPherson

The LMFBR safety research and development effort at ORNL is centered on the Fuel Failure Mockup (FFM), a sodium flow facility that has the capability of simulating LMFBR fuel subassemblies using electric cartridge heaters having prototypic configuration, power density, pressure, specific flow, and temperature. The objectives of the program include the investigation of flow and temperature distributions within fuel rod bundles with and without partial blockages to determine the potential for fuel failure and failure propagation, the detection of events that could lead to failure, and the extrapolation of experimental results to predict the behavior of the full-size reactor under hypothetical conditions.

The program consists of six parts as reported in these bimonthly progress reports. The first five are part of 189a No. 10510, Fuel Failure Mockup Facility, and the sixth is funded under 189a No. 10278, Electric Heaters for Fuel Pin Simulation.

During this reporting period, coordination has been maintained with HEDL, ANL, WARD, and RRD. A test was performed to investigate whether the FFM would experience an increase in flow impedance during isothermal operation at 1100°F as was observed in CCTL and JOYO. A HEDL representative was present during the tests, and a sodium sample was sent to HEDL for analysis. The test program for bundle 3A was temporarily interrupted to permit initiation of tests on bundle 5A. Local boiling experiments with bundle 3A were postponed.

The adaptation of the FFM for 37-pin operation at 12.5, 17.5, and 19.5 kW/ft (for 3-ft-long heated lengths) was evaluated with the recommendation that capacity be expanded to 17.5 kW/ft (∿2.0 MW total power).

The first draft of a review of the effects of partial blockages in rod bundles, intended as a backup document for the FFTF FSAR, was completed and sent to RRD, HEDL, and WARD for comments.

An expedited purchasing procedure was established for procuring boron nitride for fuel-rod-simulator heaters. Since Union Carbide is the sole source of boron nitride having acceptable properties, normal procurement

must undergo special AEC review. This expedited procedure will allow acceptable turnaround times for the heater development program.

A meeting was held with GGA representatives to discuss the feasibility of constructing an FFM-type rig for gas-cooled fast breeder fuel heat transfer experiments.

The United Kingdom engineering components team visited ORNL on June 8, 1973, and, in our opinion, a worthwhile mutual exchange of information took place.

An incident report was issued to report the failure of an Alumel heater internal thermocouple in bundle 5A. Annealing after cold work causes excessive grain growth which results in extremely brittle material.

A review meeting on the FFM and heater development program was held on June 27 and 28, 1973, and attended by RRD and HEDL. Agreements and commitments were arranged which will have a significant impact on the future course of the FFM project.

---

2. ANALYSIS AND DATA EVALUATION

M. H. Fontana L. F. Parsly
T. S. Kress J. L. Wantland

Results of Bundle 3A Experiments

The Fuel Failure Mockup (FFM), a sodium heat transfer facility, was operated with bundle 3A, which had its central six channels blocked by a 1/4-in.-long nonheat-generating stainless steel device brazed to the central rod. This section discusses the results of some of the tests using this bundle.

Test Section Arrangement

The test section for the bundle 3A experiment was arranged as shown in Fig. 2.1. The bundle was inserted from the bottom of the test section with the free ends of the heaters facing upward. This allowed the use of

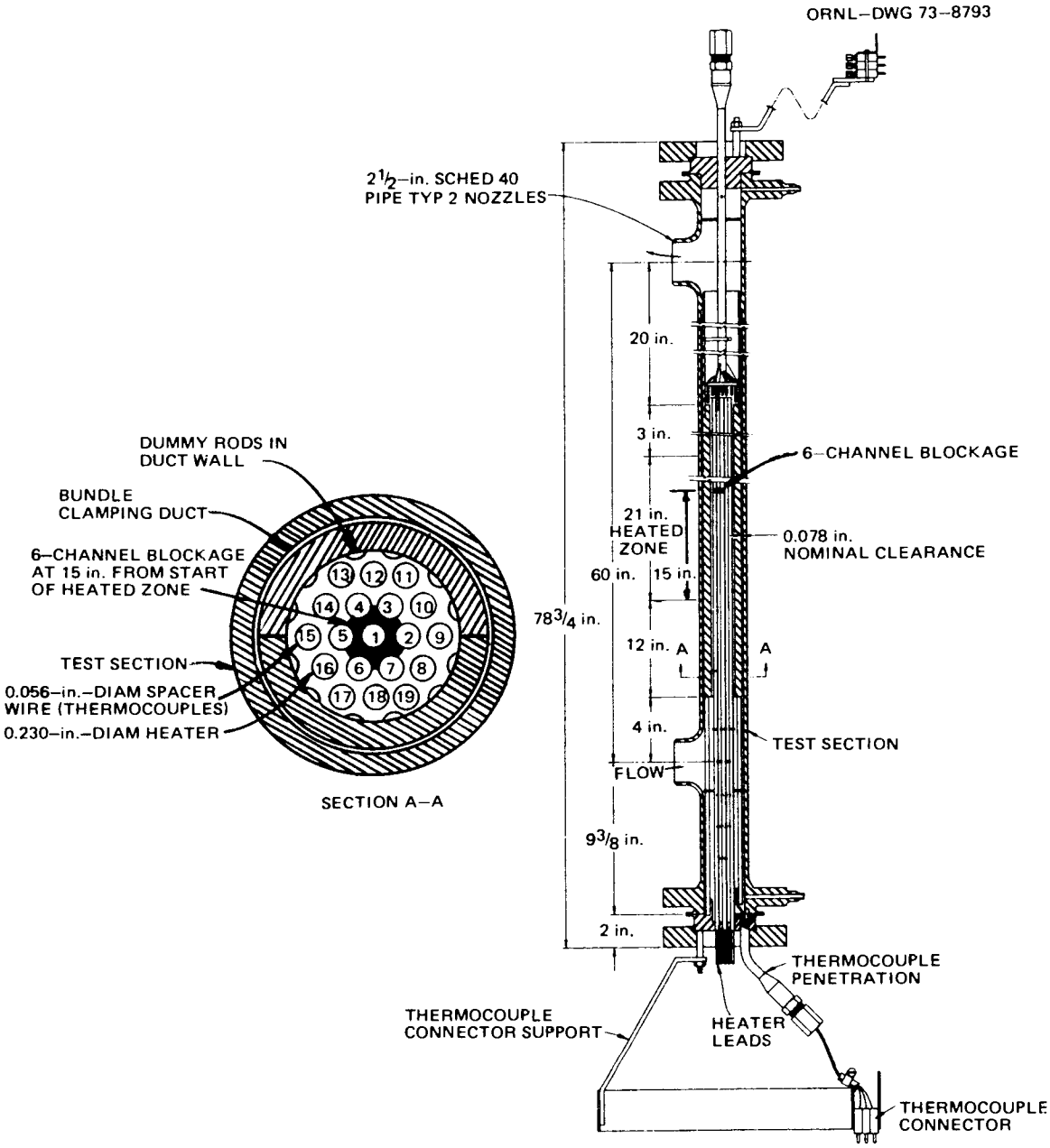

Fig. 2.1. Vertical cross section of FFM bundle 3A.

a thermocouple rake, entering from the opposite end of the test section, to monitor exit temperature from selected flow channels.

Rod bundle instrumentation

The instrumentation layout is shown in Fig. 2.2. The large circles represent the heaters that simulate the fuel rods. These are identified

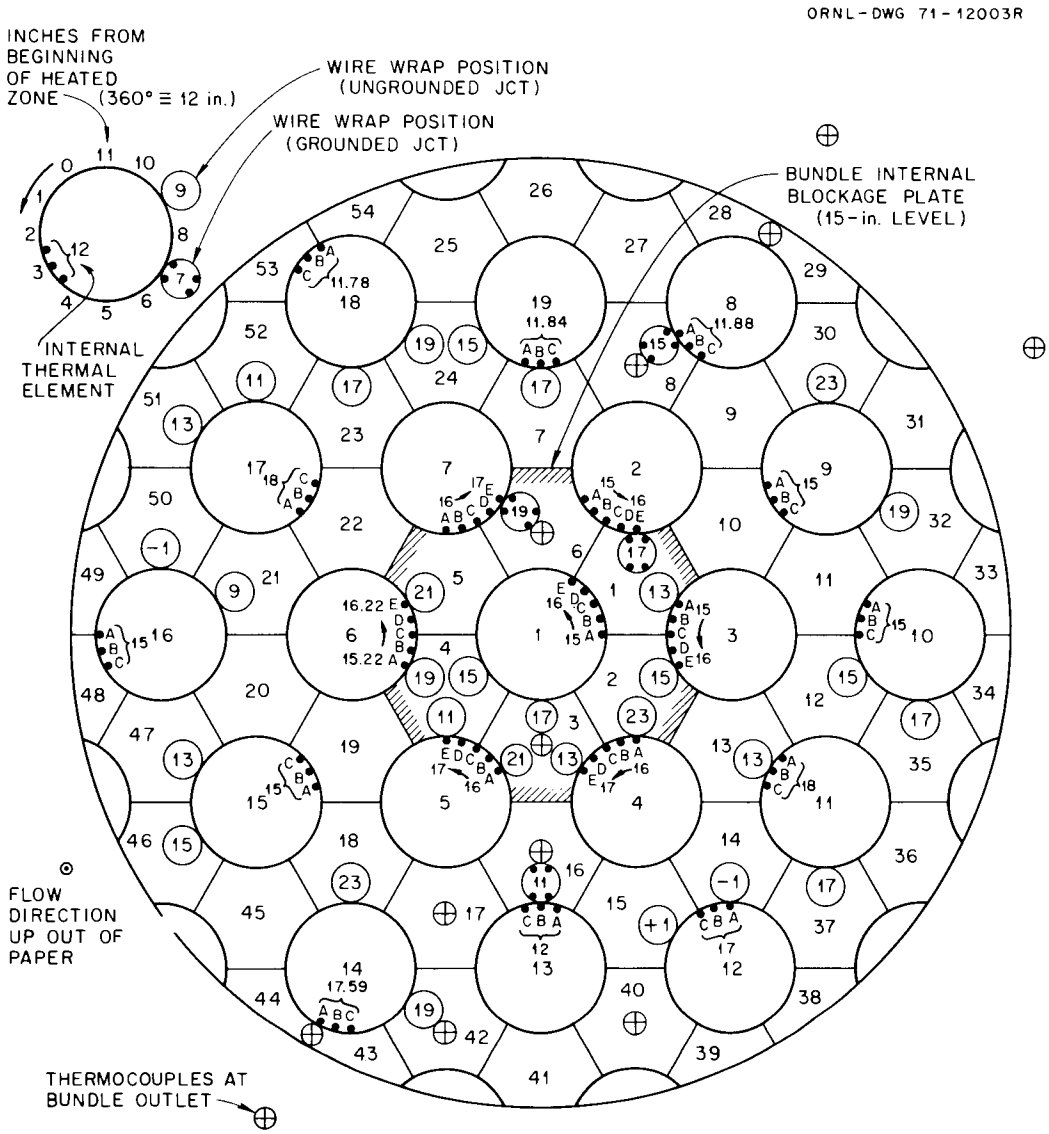

Fig. 2.2. Spacer wire and internal thermocouple locations for FFM bundle 3A.

by the central number. The small tangent circles indicate thermocouple junctions at the indicated azimuthal position of the wire-wrap spacers. The junctions are located at an axial level indicated by the numbers in the small circles, which have units of inches from the start of the heated zone. The small circles containing pairs of dots indicate the location of grounded-junction thermocouples. The pair of dots next to the heater

surface indicates that a thermocouple junction in the wire wrap is adjacent to the heater, whereas the pair of dots on the opposite side indicates that the other junction, at the same axial level, is measuring temperatures near the center of the flow subchannel. The flow subchannels, defined by the lines connecting the centers of the heaters, are identified by the numbers in the triangles so defined. The small circles with interior crosses indicate channels that are monitored by exit thermocouples.

The fuel-rod-simulator heaters have thermal elements attached to the inner surface of the cladding as indicated by the dots labeled A, B, C, etc., in the large circles. The ends of these thermal elements were grounded to the inner surface of the cladding at 15° azimuthal intervals and 0.25-in. axial intervals; thus the junction formed by two thermal elements measures an average temperature along the spiral path on the inner surface of the cladding between the two junctions. Notice that the thermal elements in heaters 1, 2, and 3 measure temperatures from 15 to 16 in. (from the start of the heated zone) in 1/4-in. increments, those in heater 6 measure from 15.22 to 16.22 in., and those in heaters 4, 5, and 7 measure from 16 to 17 in.

Experiments Performed

At the time of this writing, five sets of experiments have been performed (out of six planned). These experiments included cases with no power; all rods heated at powers of 5, 7.5, and 10 kW/ft; flows of 54, 43.2, and 32.4 gpm (100, 80, and 60% of specific FFTF full flow); rods heated singly at 8 and 10 kW/ft and 54 and 11 (20%) gpm; central seven rods heated at 10 kW/ft and 54 gpm; and three outer rods heated at each "flat" of the hexagon defined by the outer row of rods. These tests are described in Ref. 1.

This discussion will be restricted to the experiments performed at 100, 80, and 60% of full flow and 10 kW/ft because the power is higher than the FFTF average of 7.5 kW/ft, and they include the base case of

---

1. M. H. Fontana, *LMFBR Safety and Core Systems Programs Progress Report for January–February 1973*, ORNL-TM-4148 (June 1973).

full flow in addition to a flow considerably smaller than would be allowed at full power. The experimental results were selected from a sequence shown in Table 2.1. The experiments were first performed in order of ascending stress on the heaters (higher power and lower flow) and then replicated in random sequence to minimize any effect of operating sequences in the results.

Multiple readings taken for each point were averaged, and standard deviations were computed by data handling programs.

Radial heat loss from the test section was reduced by the use of insulation and guard heaters controlled to give zero temperature gradient in the insulation next to the test section wall as measured by two thermocouples in the insulation between the test section wall and the external guard heaters. Previous experiments[2] with bundle 2A indicated that extreme variations in guard heat settings did not affect experimental results significantly.

Results

The results are presented in four ways: (1) $T - T_{inlet}$ of thermal elements inside the heater sheath and in wire-wrap spacers within the central six channels, (2) exit temperature distributions, (3) normalized temperatures of heater internal thermocouples, and (4) normalized temperatures of selected wire-wrap spacer and exit thermocouples.

Temperatures in the central subchannels

Central subchannel temperatures (above inlet temperature) are shown in Figs. 2.3, 2.4, and 2.5 vs distance from the start of the heated zone. These temperatures were measured by thermocouples inside the central seven heaters and by the wire-wrap thermocouples in the central six subchannels.

The temperatures measured by the thermocouples inside the heaters are shown as horizontal lines extending the axial distance between the two thermal elements that make up the particular thermocouple being

2. M. H. Fontana et al., *Temperature Distribution in the Duct Wall and at the Exit of a 19-Rod Simulated LMFBR Fuel Assembly (FFM Bundle 2A)*, ORNL-4852 (April 1973).

Table 2.1. Experiments performed with FFM bundle 3A with power on all 19 heaters (series IV, test 2)

Purpose: To measure the effect of flow and power on bundle performance

Control:

Run	Test section			
	Flow (gpm)	Power		Heaters
		kW/ft	kW/rod	
101	54	10	17.5	All
109	32.4	5	8.75	All
106	43.2	5	8.75	All
102	54	7.5	13.13	All
108	32.4	7.5	13.13	All
105	43.2	7.5	13.13	All
107	32.4	10	17.5	All
103	54	5	8.75	All
104	43.2	10	17.5	All

Measure: Test section outlet temperature, °F
Spacer wire temperatures, °F
Heater internal temperatures, °F
Test section inlet pressure, psig
Test section outlet pressure, psig

Special instructions:

Runs to be performed in the order listed

Project management to evaluate results from tests 101 through 109 before proceeding to duplicate tests

Duplicate tests:

Run	Test section			
	Flow (gpm)	Power		Heaters
		kW/ft	kW/rod	
118	32.4	5	8.75	All
112	54	5	8.75	All
115	43.2	5	8.75	All
117	32.4	7.5	13.13	All
113	43.2	10	17.5	All
116	32.4	10	17.5	All
114	43.2	7.5	13.13	All
110	54	10	17.5	All
111	54	7.5	13.13	All

plotted. This distance is usually 1/4 in., and the indicated temperature can be considered as an average along that length. The number with the line indicates the rod within which that particular thermocouple resides. The outer cladding surface temperature was computed by subtracting a temperature drop across the cladding calculated for the given heat flux assuming radial heat flow (the latter assumption should be valid everywhere except directly underneath the blockage device). These computed outer cladding surface temperatures are indicated in the figures by the letter c.

Temperatures measured by thermocouples in the wire-wrap spacers are plotted and labeled so that the first two digits indicate the heater to which the wire-wrap spacer is attached. The second two digits indicate the axial distance downstream from the start of the heated zone, and the last digit indicates the channel in which the spacer resides at that particular axial elevation. Grounded-junction thermocouples in the wire-wrap spacers indicate two temperatures at the same elevation, one near the heater surface and the other near the center of the flow subchannel. These are also plotted.

The 90% confidence limit bands (2σ) are not shown because of their small and relatively constant values. Except for internal thermocouples 0115AB (see Fig. 2.2), which had a standard deviation σ of 3.1°F for the worst case, and 0115DE, for which σ was 3.7°F, all other internal thermocouples had σ's of about 0.3 to 1°F. The standard deviation of the wire-wrap thermocouples was about 0.5°F.

<u>Run 101 (10 kW/ft, 100% flow)</u>. Run 101 is of particular interest because it represents the case of 100% of FFTF specific flow (54 gpm for 19 rods) and a power of 10 kW/ft, which is significantly above the average FFTF linear power density. Selected measurements for this case are shown in Fig. 2.3. The abscissa starts at 13 in. from the start of the heated zone because all information of interest is downstream of this point. The blockage plate was at the 15-in. level. Estimated lengths of the recirculation zone are about 12 times the height of the step formed by the blockage plate and the central rod. Several investigators have indicated that the recirculation zone for flow over a step is between 5.2

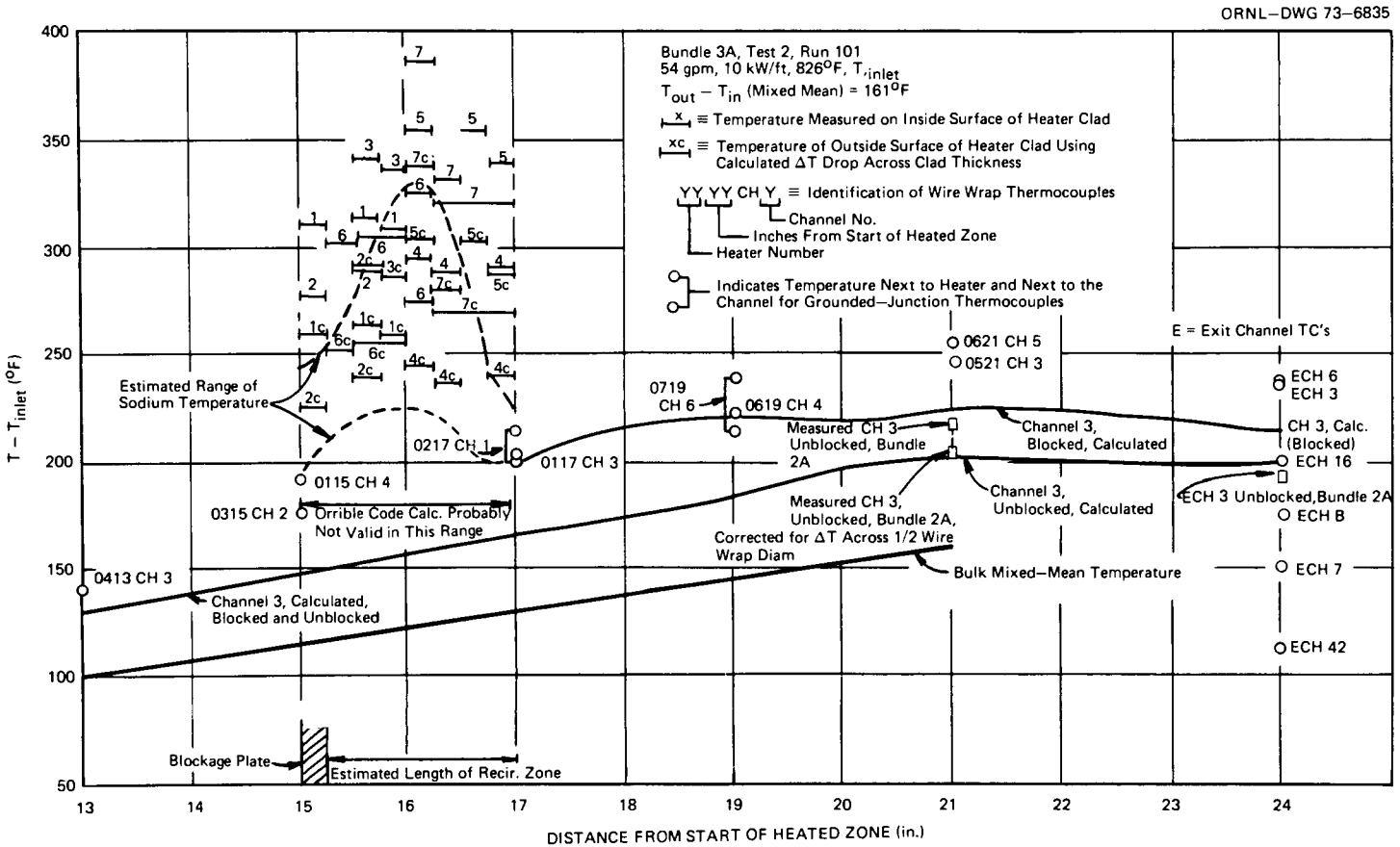

Fig. 2.3. Temperatures along the central six channels, bundle 3A (100% flow, 10 kW/ft).

and 17 times the height of the step.[3,4] The first value is for flow over a sharp edge disk in a free stream, and the second is for flow over a sharp edge wall on a flat plate. Other configurations have intermediate values.

Figure 2.3 also shows bulk mixed-mean temperature rises calculated by heat balances. At the plane of the blockage the highest measured temperature (rod 7 at 16 to 16.25 in.), adjusted to give the external cladding temperature, is approximately 200°F higher than the mixed-mean temperature at that point. However, it is not quite valid to use the mixed-mean temperature as a base for comparison because temperature peaking would also exist in the center of unblocked rod bundles.

To compare with a more realistic temperature for the unblocked case, the calculated temperature for channel 3 of unblocked bundle 2A, run 1109 (54 gpm, 10 kW/ft), is shown in Fig. 2.4 along with some pertinent experimental data points. These were calculated using the ØRRIBLE code with parameters $C_T = 0.005$, $C_D = 0.6$, and $C_S = 1.0$, where C_T is a parameter related to the turbulent mixing between subchannels, C_D is related to the pressure diversion crossflow, and C_S is related to the sweeping of fluid by the spiral wire-wrap spacers. (See Ref. 5 for a definition of these parameters.) Calculated temperatures are most sensitive to C_S and are relatively insensitive to the other two coefficients. One might infer from Fig. 2.4 that the temperature of channel 3 for the unblocked case as calculated by ØRRIBLE should be a reasonably good reference for comparison of the blocked results of bundle 3A.

---

3. A. A. Bishop, John Graham, and J. A. Zoubek, "Hydrodynamic Characteristics of a Wake Behind a Fuel Assembly Local Flow Blockage," *Trans. Amer. Nucl. Soc.* 14(2), (Oct. 17–21, 1971).

4. R. M. Roidt and Y. S. Tang, *Air Flow Measurements on a Simulated LMFBR Seven-Rod Bundle*, Part II, *Measurements of Velocities Downstream of Blocked Subchannels*, Westinghouse Scientific Paper 72-7E9-MIXIN-P1, Jan. 17, 1972.

5. J. L. Wantland, *ØRRIBLE – A Computer Program for Flow and Temperature Distribution in LMFBR Fuel Rod Bundles*, ORNL-TM-3516 (October 1971).

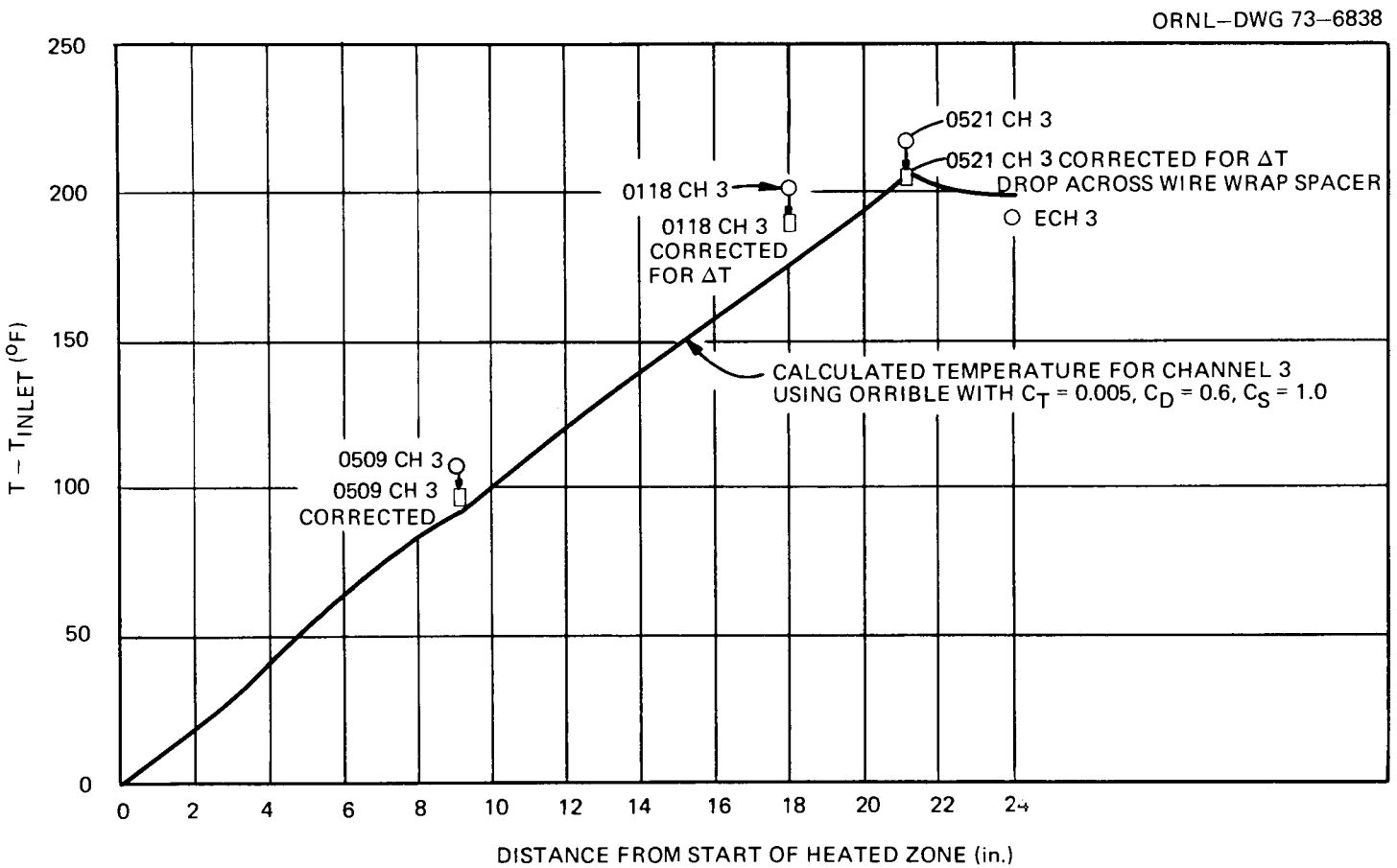

Fig. 2.4. Measured and calculated temperatures for channel 3 in unblocked bundle 2A, run 1109 (54 gpm, 10 kW/ft).

The calculated axial temperature distributions of channel 3, if it were unblocked, are shown in Fig. 2.3. The cladding outer surface temperatures appear to be about 80 to 100°F above the unblocked channel average temperature at the 15- to 17-in. level. The hottest temperature measured on the inner surface of the cladding was about 380°F above the 826°F inlet temperature and about 200°F higher than the unblocked sodium temperature at the elevation of the thermocouple (16 in.). Figure 2.3 also shows the temperatures measured by the ungrounded wire-wrap spacers in the central six subchannels: 0413 CH 3 (heater 4, 13 in. from start of heated zone, channel 3), 0115 CH 4, 0315 CH 2, 0117 CH 3, 0619 CH 4, 0621 CH 5, and 0521 CH 3. Also plotted are the grounded-junction thermocouple readings that show the radial temperature difference across the wire-wrap spacers: 0217 CH 1 and 0719 CH 6. These indicate that the ΔT's across the wire wraps are about 15°F (0217 CH 1) to 25°F (0719 CH 6). Since the ungrounded thermocouple junctions are approximately in the center of the wire-wrap spacer, a rough estimate can be made for sodium channel temperature by subtracting half the ΔT obtained with the ungrounded-junction thermocouples. Adjusted readings (plotted in Fig. 2.3) are compared with ØRRIBLE predictions for temperatures in channel 3 (since all six central channels do not deviate greatly) in the blocked configuration. Apparently the prediction of temperatures downstream from the blockage are quite good for our purposes. Exit temperatures are also plotted in Figs. 2.3, 2.5, and 2.6, but are discussed more fully later.

The ØRRIBLE-calculated predictions are not valid in the recirculating zone, which likely is about 12 times the height of the step formed by the blockage plate and the central rod (assuming the blockage plate can be viewed as a nonsharp orifice on a base plate).[6] If it is assumed that a 10 to 20°F "film drop ΔT" exists between the cladding outer surface and the average channel sodium temperature, the temperatures in the recirculating zone could be estimated as shown by the dashed line.

It is interesting to note factors that might affect some of the measurements plotted in Fig. 2.3. Referring to Fig. 2.2, the thermal elements in rod 7 are located 1 in. upstream from the six o'clock (16-in.)

---

6. P. K. Chang, *Separation of Flow*, p. 279, Pergamon, New York, 1970.

position of the associated wire wrap and 2 in. ahead of the four o'clock position. At the 15-in. level, the wire wrap on rod 7 creates a dam between rods 6 and 7 and could "trap" hot fluid below this zone. This might be responsible for the higher temperatures indicated by rod 7.

The thermal elements on rod 5 are on a spiral that touches and crosses the spiral formed by the wire-wrap spacer on rod 1. This might be responsible for the higher temperatures indicated by rod 5.

With respect to wire-wrap location, the thermal elements in rods 1, 3, 4, and 6 appear to be relatively free of its influence. Those on heater 1 face channel 1, whereas the others face adjacent rods.

The low temperatures in heater 2 are somewhat puzzling. One possible explanation is that its wire wrap, which penetrates the blockage plate at the eight o'clock position, might be leaking sufficient fluid to depress the local temperatures.

All these second-order effects do not greatly affect the main result, that is, blockage of this shape is tolerable at full flow and power.

Run 107 (10 kW/ft, 60% flow). Run 107 is of particular interest because it represents the most severe condition imposed on the test bundle up to this time. (Approach-to-boiling tests have not been done as of this writing.) The results are plotted in Fig. 2.5 in the same manner as was done in Fig. 2.3.

For this case the cladding outer surface temperatures in the vicinity of the blockage ranged from 80 to 220°F higher than the sodium temperature in the central channels (represented by channel 3) expected for the unblocked case. The hottest cladding internal surface temperature was 1327°F, about 540°F higher than the inlet temperature of 785°F.

These results indicate that a nonheat-generating blockage of the size tested is still acceptable at 60% flow conditions.

Run 104 (10 kW/ft, 80% flow). Figure 2.6 shows results plotted for run 104 in the same manner as the previous cases.

Run 102 (7.5 kW/ft, 100% flow). Figure 2.7 represents the full flow and average power conditions for the FFTF. Notice that cladding temperatures are only 280°F higher than inlet temperature and 150°F higher than the anticipated sodium temperature in channel 3 if it were unblocked.

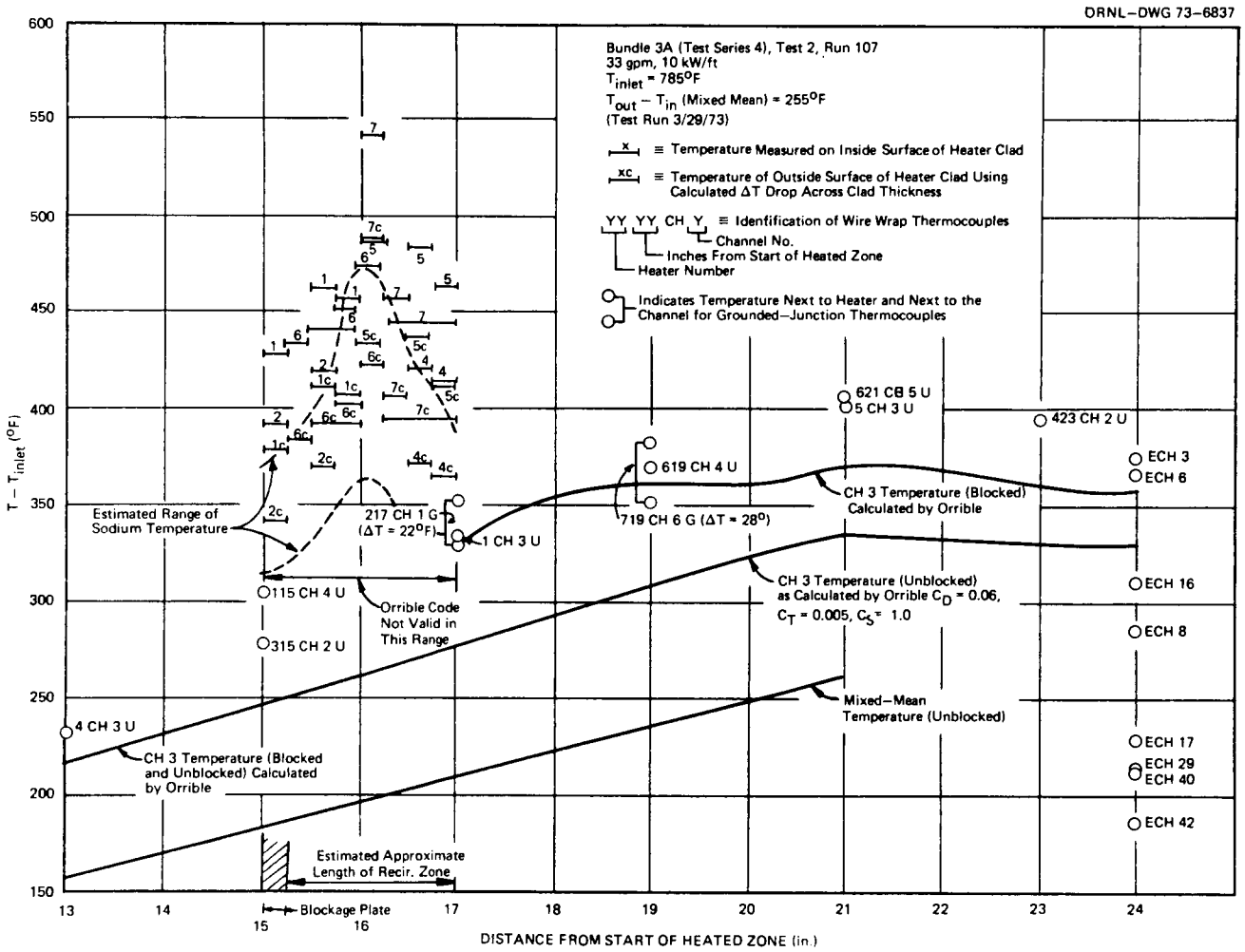

Fig. 2.5. Temperatures in six central subchannels, bundle 3A (10 kW/ft, 60% flow).

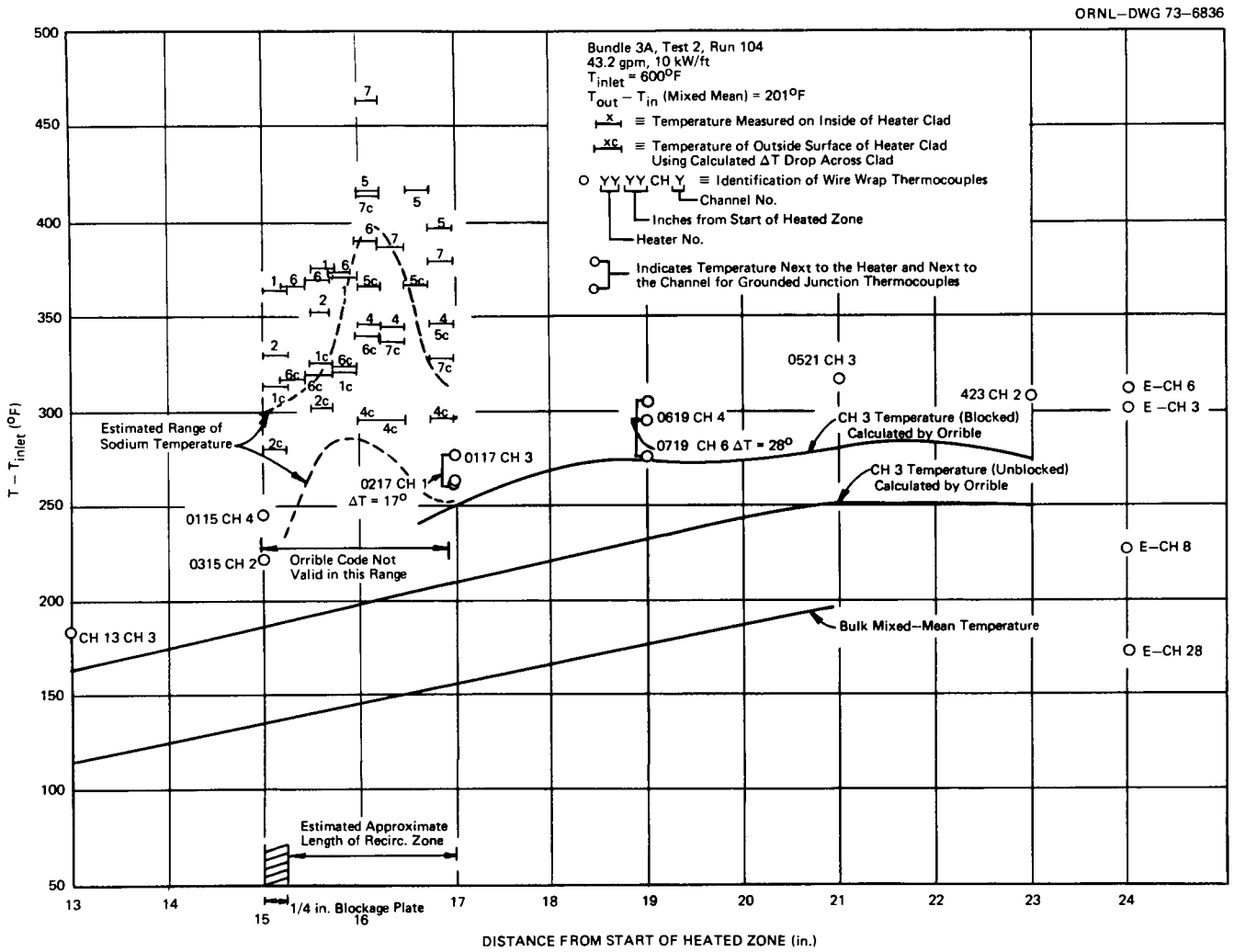

Fig. 2.6. Temperatures in central subchannels, bundle 3A (10 kW/ft, 80% flow).

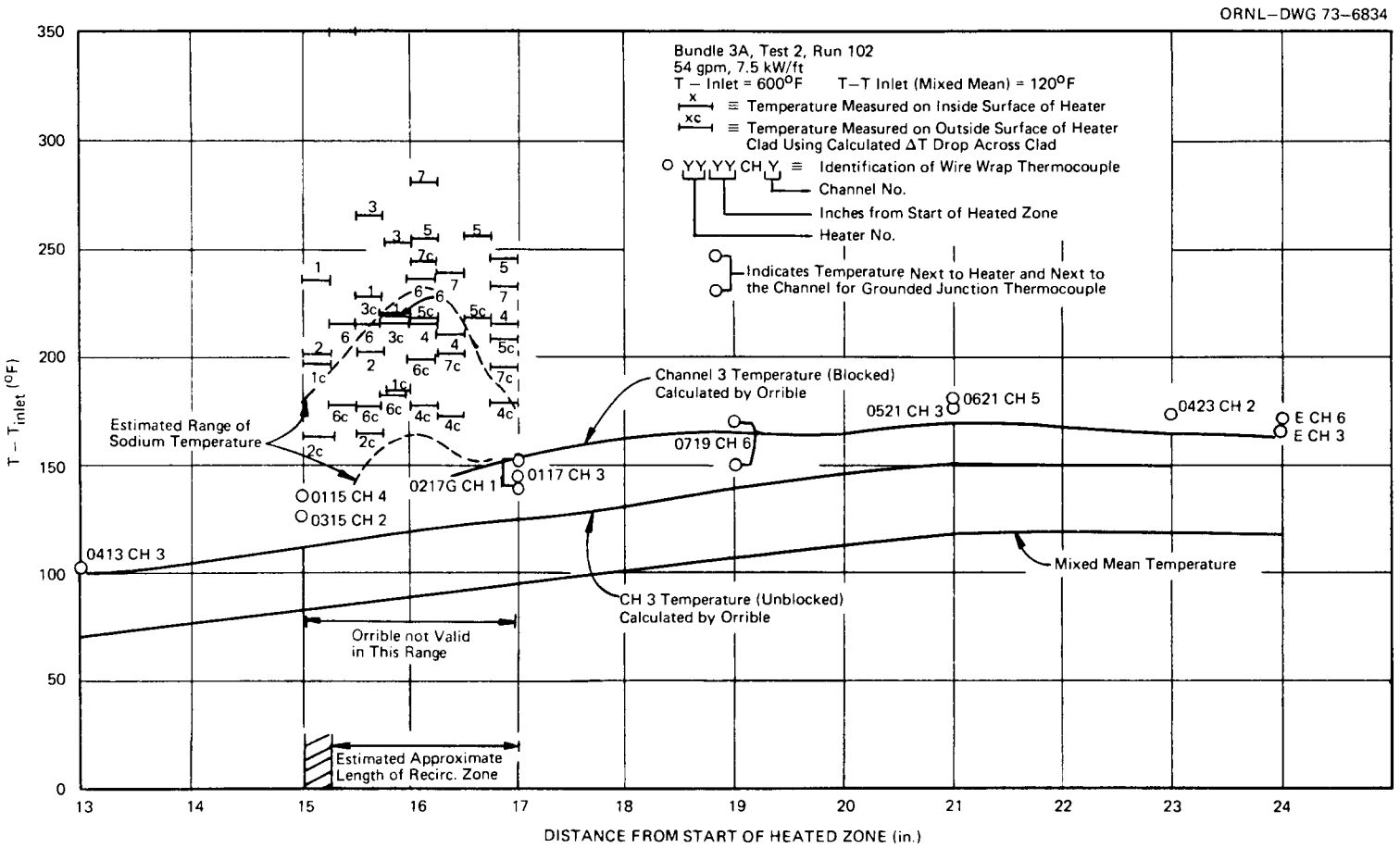

Fig. 2.7. Temperatures in central subchannels, bundle 3A (7.5 kW/ft, 100% flow).

Exit temperatures

The temperatures at the exits of selected subchannels (Fig. 2.2) were measured using the exit rake. These are valuable because they indicate a temperature that should represent the particular subchannel exit mixed-mean temperature because of the mixing that would occur in the 3 in. of unheated flow between the end of the heated zone and the channel exit. Thus, these measurements provide results that can be directly compared with analytical prediction of subchannel temperatures. In addition, they indicate the magnitude of the influence of an in-core blockage on the exit temperature profile and should then indicate the feasibility of detecting the blockage by thermal devices located in the exit plane.

To have an unblocked case exit temperature profile for comparison, a diametral traverse of the normalized temperature distribution measured in unblocked bundle 2A (10 kW/ft; 53 gpm) along with ØRRIBLE predictions for that case are plotted in Fig. 2.8 (see Fig. 2.2 for identification of channel numbers). Bundle 2A was identical to bundle 3A except that it was unblocked and had a hexagonal duct instead of a wire-wrap dummy rod

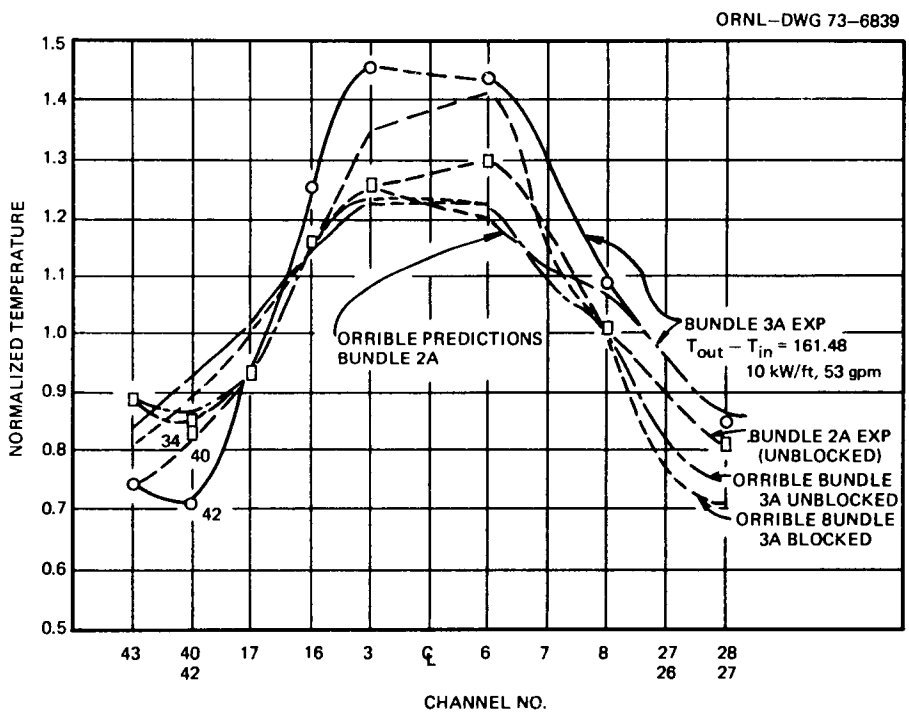

Fig. 2.8. Measured and calculated normalized exit temperatures for unblocked bundle 2A and blocked bundle 3A.

duct. The agreement (within ∿6°F) indicates that ØRRIBLE is a good predictor for that case.

Also plotted in Fig. 2.8 is the calculated normalized exit temperature distribution for unblocked bundle 3A. The agreement between the calculated and the measured bundle 2A temperature distribution indicates that the calculation may serve as a reference for comparison with the results of the blocked bundle experiments. Therefore the pertinent experimental results for bundle 3A, plotted in Fig. 2.8, show a temperature increase over the unblocked case of 0.2 unit, or 32°F. The ØRRIBLE predictions for the blocked core, shown in Fig. 2.8, show a better agreement at channel 6 (0.4 unit; ∿6°F) than at channel 3 (0.1 unit; ∿16°F).

Figure 2.9 shows the exit temperature distribution expressed as $T - T_{inlet}$ for the experimental case of 10 kW/ft and 100% flow (54 gpm) and for the pertinent calculated blocked and unblocked cases. Figure 2.10

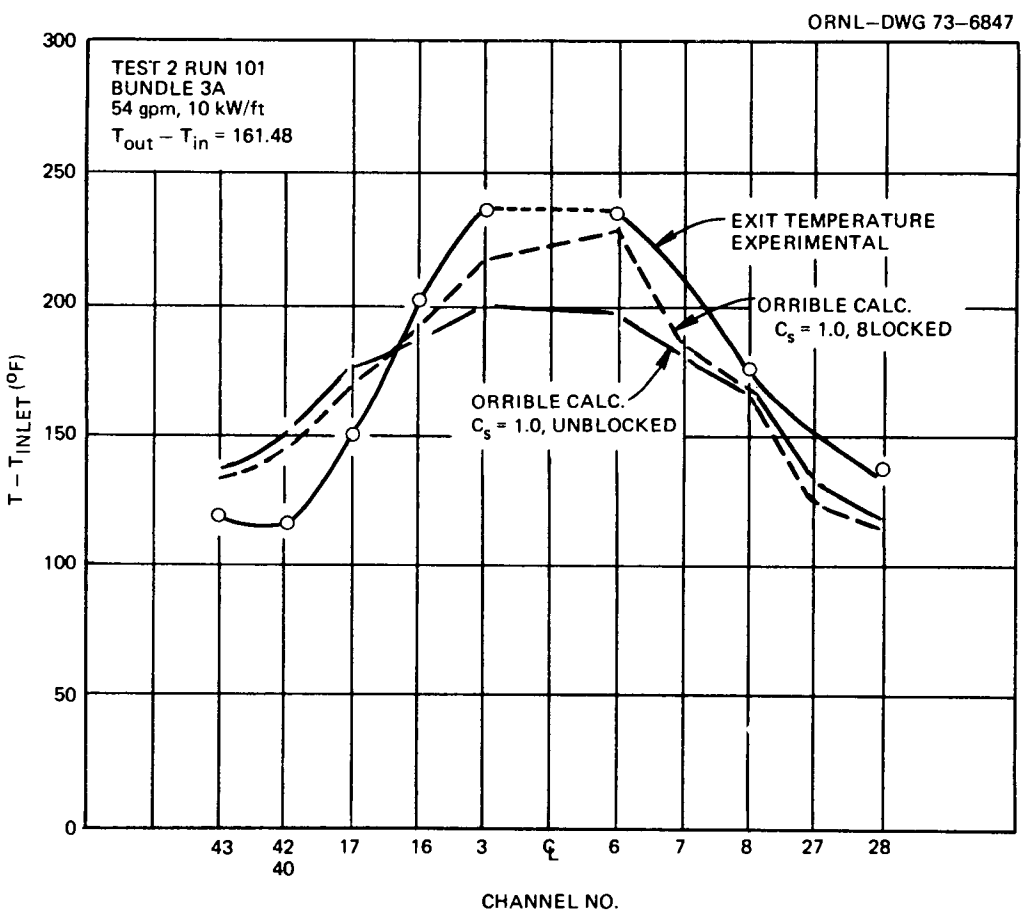

Fig. 2.9. Measured and calculated exit temperatures, bundle 3A (10 kW/ft, 100% flow).

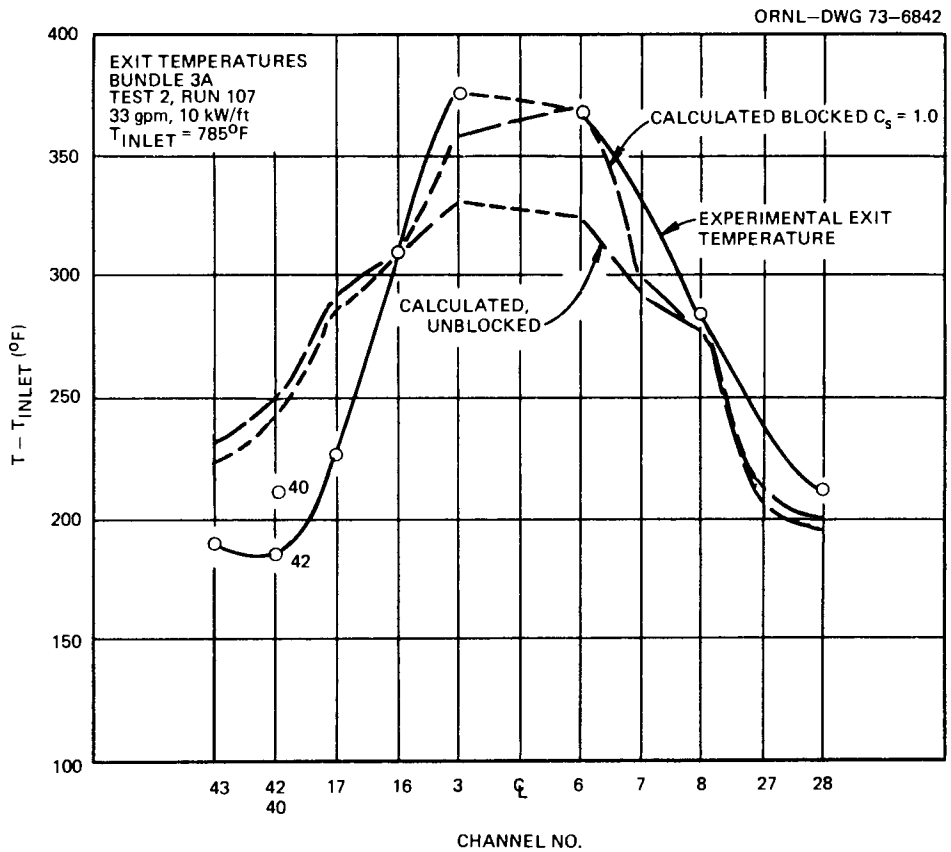

Fig. 2.10. Measured and calculated exit temperatures, bundle 3A (10 kW/ft, 60% flow).

shows similar results for the most severe case of 10 kW/ft and 60% flow (33 gpm).

The FFTF fuel has exit gas plenums of 42 in. If the FFM bundle 3A had an exit unheated length of 42 in., the temperature distribution as calculated by ØRRIBLE would be as shown in Fig. 2.11. This shows that, at least at full flow, correlation techniques on a small number of exit thermocouples per channel might detect a blockage as small as six channels with as little as 6 in. of heated zone adding heat to the perturbed flow downstream from the blockage. This observation is not of direct relevance to the present FFTF design but might be considered for future use.

Figure 2.12 shows the exit temperature distribution for the 3-in. unheated zone and for the 42-in. unheated zone for the average operating case of 7.5 kW/ft and 100% (54 gpm) flow.

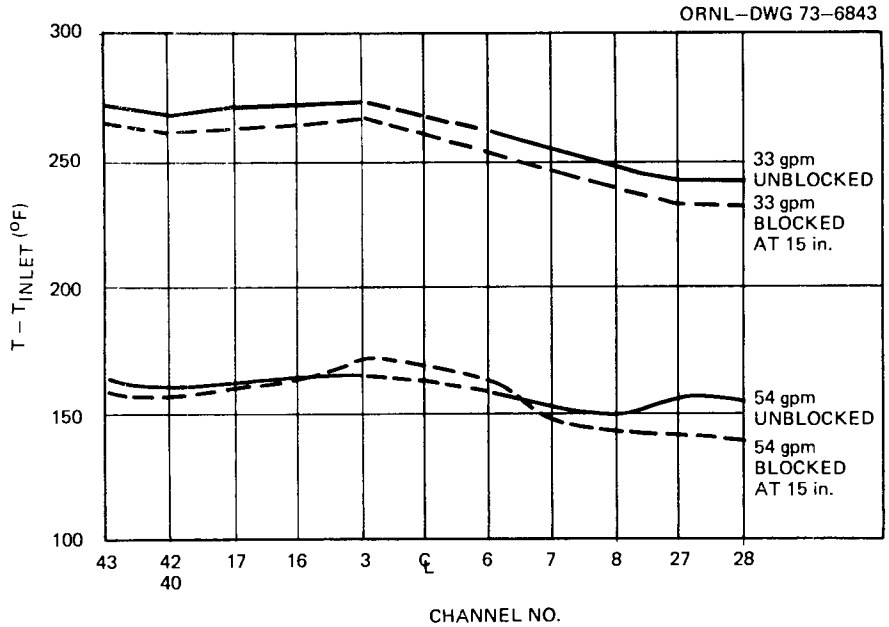

Fig. 2.11. Calculated exit temperature distribution for bundle 3A type with 42-in. exit plenum.

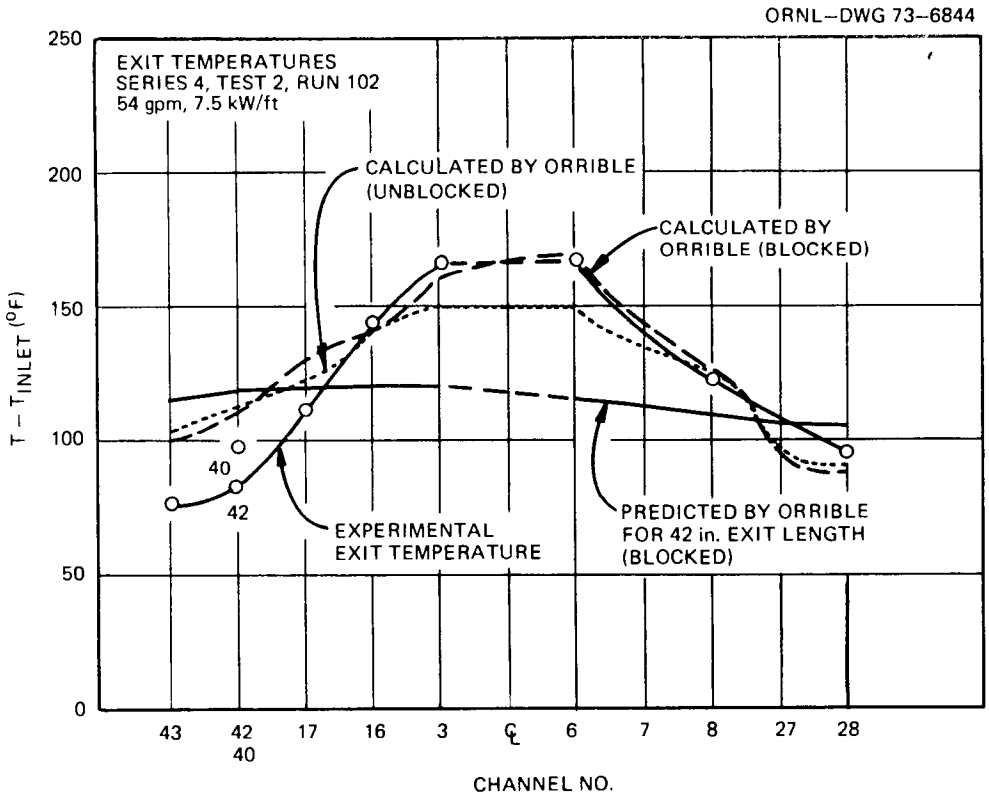

Fig. 2.12. Exit temperature distribution for bundle 3A with 3- and 42-in. exit plenums.

Normalized temperatures of heater internal thermocouples

The normalized temperatures, $(T - T_{in})/(T_{out} - T_{in})$, for all operative heater internal thermocouples are shown in Table 2.2. The highest normalized temperature (2.76) was obtained from thermocouple 0716AB (see Fig. 2.2) for the case of 54 gpm and 5 kW/ft where $T_{out} - T_{in}$ was 80°F. Because of the nonlinear relationships between the various ΔT's from the point of temperature measurement to the inlet and outlet temperatures that serve as normalization base points, the normalized temperatures are not uniform over variations of power and flow. Preliminary analysis indicates that the normalized temperatures should be less sensitive to power difference than to flow. These evaluations are continuing.

Table 2.2. Normalized temperatures of heater internal thermal elements — FFM bundle 3A, test 2

Results for internal thermal elements, FFM series IV

Run No.	101	109	106	102	108	105	107	103	104
Flow, gpm	54	32.4	43.2	54	32.4	43.2	32.4	54	43.2
Power, kW/ft	10	5	5	7.5	7.5	7.5	10	5	10
Mixed-mean temp. rise, °F	161	134	101	121	201	151	268	80	201
Description									
TC R1312BC htr. 13	a	0.477	0.659	a	0.190	0.168	a	0.423	a
TC R1812AB htr. 18	1.044	0.844	0.988	1.095	0.854	0.990	0.846	1.137	0.960
TC R1912AB htr. 19	1.377	1.168	1.318	1.428	1.190	1.327	1.185	1.482	1.304
TC R1912BC htr. 19	1.389	1.188	1.334	1.448	1.209	1.351	1.199	1.498	1.324
TC F0115AB htr. 1	1.931	1.689	1.896	2.054	1.719	1.910	1.681	2.147	1.833
TC R0116CD htr. 1	1.945	1.845	1.952	2.106	1.869	1.984	1.816	2.151	1.895
TC R0116DE htr. 1	1.916	1.731	1.860	1.955	1.782	1.902	1.793	2.015	1.876
TC R0215AB htr. 2	1.732	1.486	1.647	1.797	1.522	1.676	1.533	1.851	1.664
TC R0215CD htr. 2	1.806	1.589	1.711	1.895	1.617	1.743	1.647	1.883	1.774
TC R0316CD htr. 3	2.147	1.879	2.145	2.282	a	a	a	a	a
TC R0316DE htr. 3	2.139	1.834	2.023	2.167	a	a	a	a	a
TC R0615AB htr. 6	1.879	1.680	1.819	1.951	1.716	1.849	1.718	1.993	1.846
TC R0615BD htr. 6	1.863	1.668	1.793	1.906	1.708	1.837	1.737	2.006	1.861
TC R0616CD htr. 6	1.902	1.700	1.823	1.949	1.738	1.852	1.770	2.017	1.878
TC R0616DE htr. 6	2.019	1.809	1.952	2.080	1.840	1.987	1.858	2.086	1.967
TC R0915AB htr. 9	1.859	1.530	1.745	1.932	1.571	1.780	1.574	1.965	1.763
TC R0915BC htr. 9	1.937	1.623	1.855	2.030	1.632	1.860	1.612	2.088	1.809
TC R0416AB htr. 4	1.836	1.637	1.768	1.874	1.673	1.794	1.653	1.935	1.742
TC R0416BC htr. 4	1.802	1.596	1.746	1.851	1.645	1.780	1.628	1.915	1.737
TC R0417DE htr. 4	1.815	1.611	1.769	1.884	1.646	1.798	1.626	1.952	1.746
TC R0516AB htr. 5	2.209	1.924	2.142	2.310	1.934	2.147	1.917	2.408	2.104
TC R0517CD htr. 5	2.207	1.921	2.148	2.312	1.940	2.157	1.914	2.397	2.102
TC R0517DE htr. 5	2.112	1.828	2.032	2.220	1.840	2.048	1.819	2.292	2.000
TC R0716AB htr. 7	2.400	2.177	2.460	2.639	2.146	2.414	2.127	2.760	2.341
TC R0716BC htr. 7	2.060	1.806	2.025	2.187	1.817	2.024	1.792	2.258	1.950
TC R0717BE htr. 7	1.993	1.737	1.953	2.122	1.768	1.980	1.744	2.190	1.903
TC R1217AB htr. 12	1.511	a	a	1.570	1.327	1.468	1.320	1.598	1.445
TC R1217BC htr. 12	1.543	a	a	1.605	1.353	1.497	1.352	1.642	1.473
TC R1418AB htr. 14	1.307	1.110	1.271	1.389	1.097	1.246	1.081	1.429	1.208
TC R1418BC htr. 14	1.396	1.120	1.277	1.447	1.147	1.320	1.143	1.422	1.288

[a]Thermocouple failed.

Normalized temperatures of wire-wrap and exit thermocouples

The normalized temperatures for selected exit, ungrounded wire-wrap, and grounded wire-wrap thermocouples are given in Table 2.3. These indicate that the highest temperatures near the heaters (e.g., see TC 0719A heater 7) are of the same magnitude as the highest exit temperature (see exit channels 3 and 6). For each thermocouple the normalized results are more constant than was the case for the heater internal thermocouples because the ΔT across the cladding was not involved in the normalization.

Table 2.3. Selected normalized temperatures[a] from FFM bundle 3A, test 2

Run No.	101	102	103	104	105	106	107	108	109
Power, kW/ft	10	8	5	10	8	5	10	8	5
Flow, gpm	54	54	55	43	44	44	33	32	32
Mixed-mean temp. rise, °F	162	129	79.5	203	159	99.4	265	219	137
Description									
Exit ch. 3	1.455	1.473	1.488	1.512	1.500	1.448	1.466	1.471	1.438
Exit ch. 16	1.246	1.266	1.288	1.262	1.260	1.243	1.215	1.211	1.218
Exit ch. 17	0.938	0.972	0.966	0.930	0.940	0.950	0.891	0.910	0.938
Exit ch. 40	0.826	0.847	0.858	0.843	0.841	0.853	0.831	0.837	0.850
Exit ch. 42	0.711	0.706	0.714	0.729	0.722	0.720	0.725	0.724	0.719
Exit ch. 43	0.738	0.660	0.661	0.757	0.759	0.682	0.743	0.760	0.701
Exit ch. 6	1.473	1.481	1.496	1.562	1.517	1.460	1.534	1.504	1.435
Exit ch. 8	1.088	1.109	1.154	1.138	1.150	1.112	1.106	1.113	1.097
Exit ch. 28	0.846	0.837	0.856	0.863	0.853	0.838	0.838	0.851	0.835
TC 0117U ch. 3	1.274	1.285	1.309	1.329	1.313	1.271	1.310	1.297	1.254
TC 1017U ch. 35	1.033	1.035	1.050	1.045	1.037	1.002	1.007	0.997	0.962
TC 0619U ch. 4	1.423	1.429	1.463	1.486	1.452	1.397	1.451	1.430	1.386
TC 0919U ch. 32	0.939	0.959	0.968	0.960	0.954	0.931	0.931	0.921	0.894
TC 0521U ch. 3	1.527	1.541	1.577	1.594	1.568	1.516	1.567	1.541	1.494
TC 0423U ch. 2	1.509	1.521	1.555	1.576	1.554	1.504	1.550	1.544	1.494
TC 0815A htr. 8	1.052	1.061	1.071	1.061	1.045	1.021	1.023	1.005	0.979
TC 0815B ch. 8	0.927	0.933	0.953	0.967	0.948	0.924	0.957	0.944	0.920
TC 0217A htr. 2	1.326	1.339	1.348	1.396	1.373	1.320	1.381	1.363	1.307
TC 0217B ch. 1	1.244	1.245	1.288	1.309	1.278	1.229	1.292	1.276	1.229
TC 0719A htr. 7	1.482	1.487	1.513	1.533	1.506	1.447	1.503	1.475	1.413
TC 0719B ch. 6	1.325	1.334	1.355	1.391	1.364	1.311	1.375	1.350	1.300

[a]Normalized temperatures $\equiv (T - T_{inlet})/(T_{outlet} - T_{inlet})$.

Conclusions

Excessive temperatures are not generated in the heater rods as a consequence of a nonheat-generating blockage over an area of six subchannels in the 19-pin FFM bundle 3A even at 10 kW/ft and 60% flow. Since the blockage covers a flow area of only about 10% of the total area, one would expect that the wall effects on the flow in the vicinity of the blockage

would be small. It would also be expected that a similar nonheat-generating blockage would behave in essentially the same way in a full-size 217-pin FFTF fuel subassembly and therefore would not cause excessive temperatures. It also appears that relatively small blockages affect the exit temperature distribution to an extent that correlation techniques between various thermocouples might eventually be used to detect such anomalies.

Effect of Six-Channel Internal Blockage in a Full-Size Fuel Subassembly

The six-channel blockage tested in FFM bundle 3A is small compared with the size of the 19-pin experimental bundle. Therefore, the local temperatures measured in the vicinity of the blockage can be expected to be typical of local temperatures of identical blockages in a larger bundle. Because of the effect of the walls on the rod bundle, however, one might expect that the temperature distribution some distance from the blockage might be different in the full-size bundle.

The 217-pin version of ØRRIBLE was used to compute the temperature distributions along one of the central channels (channel 3) at the exit of the heated zone and at the exit of the 42-in. unheated length.

Figure 2.13 shows the predicted axial temperature distribution for channel 3 for the unblocked case and the case where the blockage exits 6 in. from the exit end of the heated zone. This position was chosen because comparison could be made with bundle 3A, which had the same length over which heat could be added to the perturbed flow (thereby acting as a tracer) prior to leaving the bundles. The temperature in the zone 2 in. downstream of the blockage was inferred from bundle 3A experimental results.

Fig. 2.14 shows the calculated temperature distribution plotted across the exit of the 217-pin bundle. The abscissa is in terms of channel numbers that identify the channels from the 11 o'clock corner of the rod bundle to the 5 o'clock corner. This shows a temperature spike of about 90°F, which is considerably hotter than the 20°F indicated by bundle 3A. A possible reason for this might be the effect of mixing with cooler wall subchannels on bundle 3A at distances far downstream from the blockage.

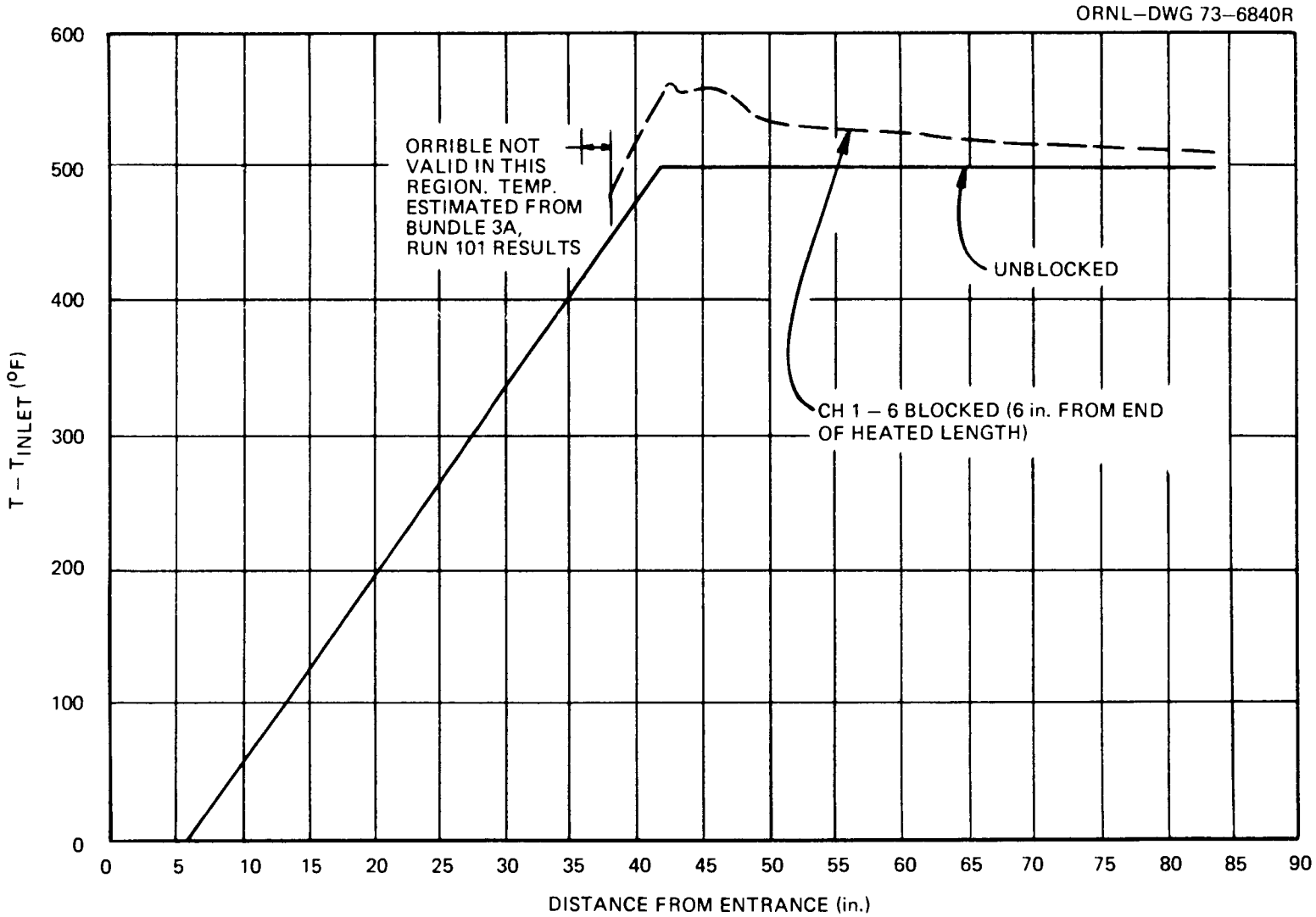

Fig. 2.13. Calculated temperature distribution in channel 3 for 217-pin bundle (10 kW/ft, 100% flow).

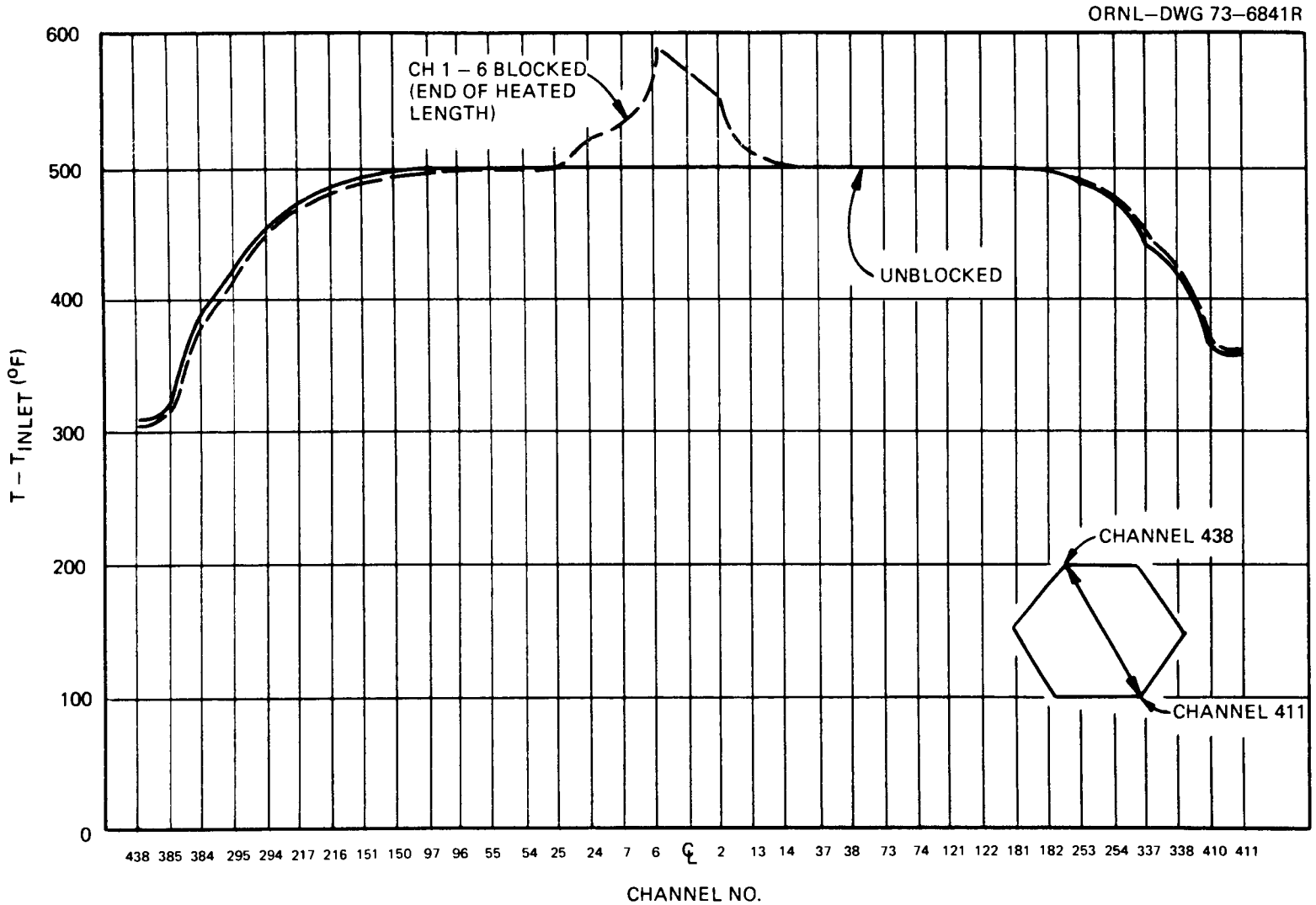

Fig. 2.14. Calculated temperature for 217-pin bundle, end of heated zone.

Fig. 2.15 shows the temperature distribution, plotted as in Fig. 2.13, at the exit of the rod bundle after the flow had traversed 42 in. of unheated zone representing the exit reflector and fission gas plenums. This figure shows that the blockage would perturb the exit temperature distribution by about 10°F, although the exit mixed-mean temperature would remain the same. This indicates that FFTF exit instrumentation, since it measures mixed-mean temperature, could not detect the six-channel blockage, but a future system using several thermocouple and cross-correlation techniques might detect changes in temperature distribution caused by this size (and larger) blockage.

Status of ØRRIBLE Code Versions

There are presently eight operable versions of ØRRIBLE: five for 19-rod bundles and three for 37-, 91-, and 217-rod bundles respectively. For the latter three versions, the name is followed by a hyphen and the number of rods considered, for example, ØRRIBLE-37 is for a 37-rod bundle. For all versions, the name is followed by a six-digit number indicating the date on which that version was first compiled. For example, ØRRIBLE 040672 was compiled on April 6, 1972. If any changes are made to a particular version, the compilation date is also changed.

A brief description of these eight versions of ØRRIBLE follows; a detailed report covering these changes is in preparation.

ØRRIBLE 040672. This is the corrected version of ØRRIBLE 081271 reported in ORNL-TM-3516. It is for 19 rods in a hexagonal duct with right-hand helical wire wraps (FFM bundle 2). Seven errors in the referencing arrays reported were corrected. These are

J3(33) = 43 [not 34],
J1(6) = 5 [not 1],
J2(6) = 1 [not 5],
J1(24) = 23 [not 7],
J2(24) = 7 [not 23],
J2(25) = 42 [not 26],
J3(25) = 26 [not 42],

Several minor formatting changes were made, but operationally ØRRIBLE

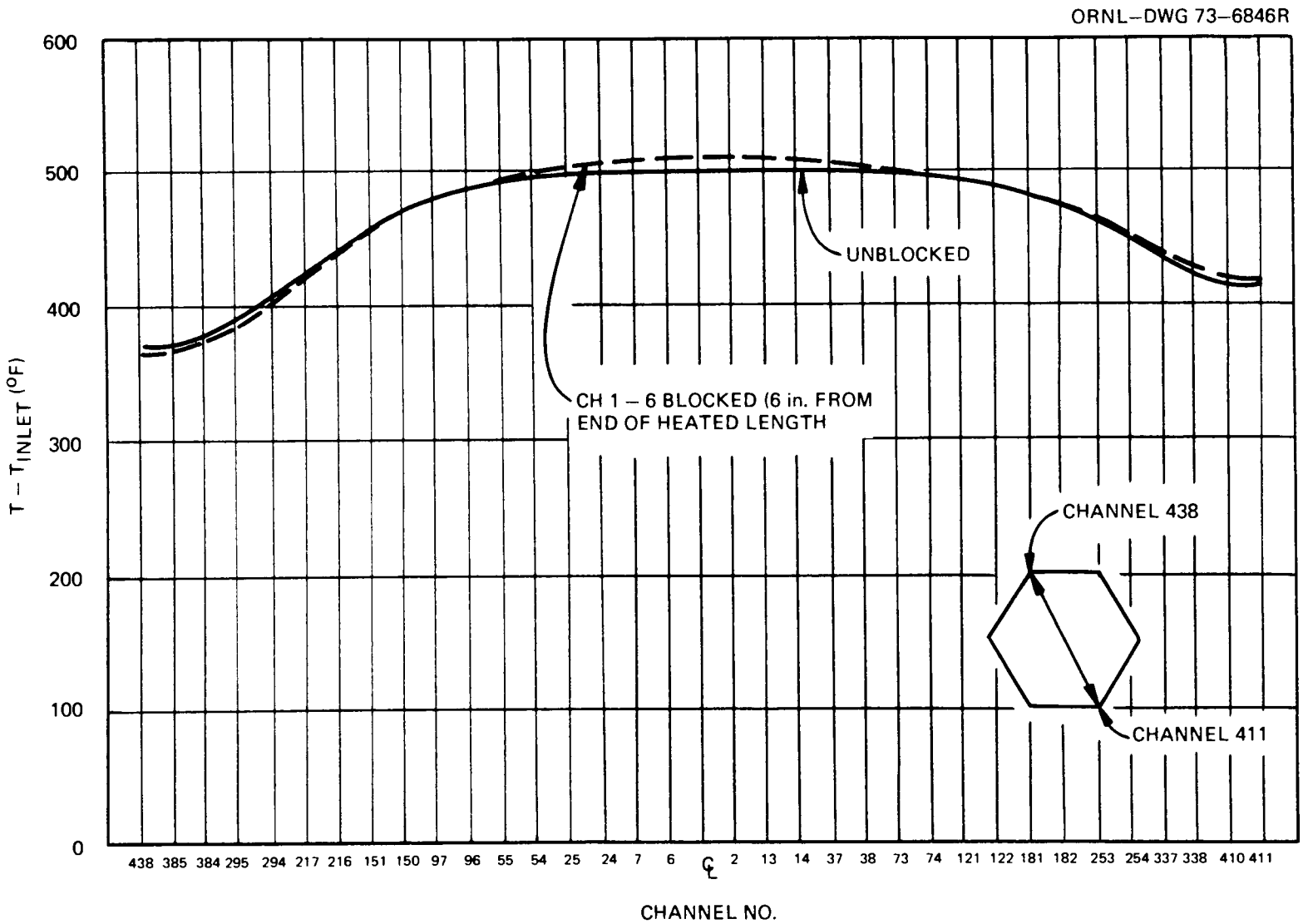

Fig. 2.15. Calculated temperature for 217-pin bundle, end of 42-in. exit plenum.

040672 is identical to that reported in ORNL-TM-3516 (with the above errors corrected).

ØRRIBLE 120572. This is based on the previous program with the addition of four input parameters to improve the versatility of the program. (1) AWH is an input parameter that specifies the effective potential orientation of the wire wraps at the start of the heated section. There are indications that the angle of maximum sweeping crossflow may not coincide exactly with the location of the wire wrap. This may be modeled by varying the value of AWH. (2) CE specifies the sweeping crossflow coefficient for the edge gaps only (i.e., those contiguous to the hexagonal duct wall). (3) AG specifies the angle of influence of the wire wraps in the edge gaps. (The angle of influence of the interior gaps is 120°.) By setting AG = 0.0, edge-gap wire-wrap sweeping is uniform (i.e., not a function of local wire-wrap orientation). (4) EG specifies the ratio of the edge-gap dimension to that of the interior gap. By specifying EG = 0.5, the configuration of the FFM bundle 5 is specified for which the edge-gap thickness is one-half that of the interior gaps. By specifying AWH = 1.0, CE = CS, AG = 2.0, and EG = 1.0, computation identical to that of ØRRIBLE 040672 is performed.

ØRRIBLE 031273. This version is for the same configuration, 19 rods in a hexagonal duct. The fundamental equations had been rederived to take into consideration the variation in channel cross-sectional areas as the wire wraps move through the gaps to model the effect referred to as "wire-wrap pumping." Channel cross-sectional area as a function of length is computed in a new subroutine called VAREAS, which contains the input parameters AWH, CE, and AG previously described.

It had been suggested that with the helical wire wraps installed, due to initial wire-wrap tension and further thermal differential expansion, the heater rods do not remain straight during operation but each heater rod—wire-wrap pair forms a configuration similar to that of a twisted pair of wires. Thus the rod bundle itself would form a helix in the hexagonal duct. To model this possibility, it is necessary to consider a variation in cross-sectional area of the edge channels. Hence

in this version of ØRRIBLE an input parameter DY is provided which specifies the radius, in feet, of the bundle helix in the duct (DY = 0.0 specifies a straight bundle).

The computational details of this version will be described in the forthcoming topical report.

ØRRIBLE 040772. This is for a 19-rod bundle in a scalloped duct with the wire wraps forming a left-hand helix. This is the configuration of the FFM bundle 1, the only configuration in which the wire wraps form a left-hand helix. Computationally, ØRRIBLE 040772 is the same as ØRRIBLE 040672.

ØRRIBLE 040872. This is for a 19-rod bundle in a scalloped duct with dummy wire wraps on the dummy edge rods, the configuration of FFM bundle 3. Computationally, ØRRIBLE 040872 is the same as ØRRIBLE 040672.

ØRRIBLE-37 031473. This is for a 37-rod bundle in a hexagonal duct (FFM bundle 4). Computationally, it is identical to ØRRIBLE 031273 with the subroutine VAREAS.

ØRRIBLE-91 012373. This is for a 91-rod bundle in a hexagonal duct. It is computationally identical to ØRRIBLE 120572, except that the input parameter EG is not available. The edge gaps have the same thickness as the interior gaps.

ØRRIBLE-217 041272. This is for a 217-rod bundle in a hexagonal duct (FFTF configuration). It is computationally identical to the original 19-rod version ØRRIBLE 040672.

For all these versions of ØRRIBLE, although the linear heat rate for each rod is individually specified, variation in axial heat-generation rate is not provided. Consideration is being given to include this option (e.g., as a chopped-cosine distribution) in future versions of the program.

---

3. WATER SYSTEM MOCKUP OF THE FFM FACILITY

D. G. Thomas R. B. Heimdahl

Heated-zone edge blockage tests were continued with the FFM water mockup (linear dimensions 3 × FFM scale). For these tests, the spacing

between the 12 peripheral rods of the 19-rod bundle and the walls of the hexagonal duct is one-half of the normal distance of 0.165 in. To accomplish this, the walls of the Plexiglas duct were lined with 85-mil-thick Plexiglas shims, which were bonded with a dichloroethane-Plexiglas mixture. A nickel heater tube is installed in a corner of the rod bundle, and a Plexiglas rod is installed as the center rod of the bundle. The spacer wire on each of the outer rods was machined flat at each position corresponding to a point of contact with a duct wall. This was done so that the spacing distance between the outer rods and the duct walls is 80 mils, while the normal spacing distance of 0.165 in. between rods is maintained.

A 1/4-in.-thick heated-zone edge blockage plate was installed in the rod bundle with the blockage plate center (BPC) located 9 in. from the start of the heated length, or 27 in. above the bundle base. The flow area blocked is one-third of the total flow area. With the blockage plate located at this position, the wire wrap on the heated rod is in contact with the channel side walls from 5 1/2 to 13 in. downstream of the blockage plate. This means that channel-to-channel crossflow on the periphery of the bundle is possible both upstream of the blockage plate and for 5 1/2 in. downstream of the blockage plate.

Test conditions for the runs conducted with the edge blockage plate are given in the following table.

Test No.	Average velocity (fps)	N_{Re}	Heat flux [Btu hr^{-1} ft^{-2} $(^{o}F)^{-1}$]
58-D	10	2.5×10^4	4.9×10^4
59	10	2.6×10^4	4.9×10^4
60	28.1	9.4×10^4	6.8×10^4
61[a]	9.5	2.4×10^4	5.4×10^4
62[b]	10.3	2.6×10^4	7.5×10^4

[a]A slight leak was present between the blockage plate and the channel wall.

[b]The leak from the previous test was substantially increased.

At the conclusion of test 62, the edge blockage plate was removed and the tube bundle returned to the reference condition to check the results of tests 53 to 56. The conditions for these tests are given below.

Test No.	Average velocity (fps)	N_{Re}	Heat flux [Btu hr^{-1} ft^{-2} $(°F)^{-1}$]
63	10.3	2.63×10^4	2.9×10^5
64	4.46	1.13×10^4	1.2×10^5
65	19.4	4.8×10^4	3.3×10^5

The circumferential variation of heat transfer coefficient for the unblocked reference bundle is shown in Fig. 3.1 for various locations along the heated rod. For convenience, the locations (−6, 0, +3, +9, +12, and +24 in.) are given with respect to the location of the edge blockage plate

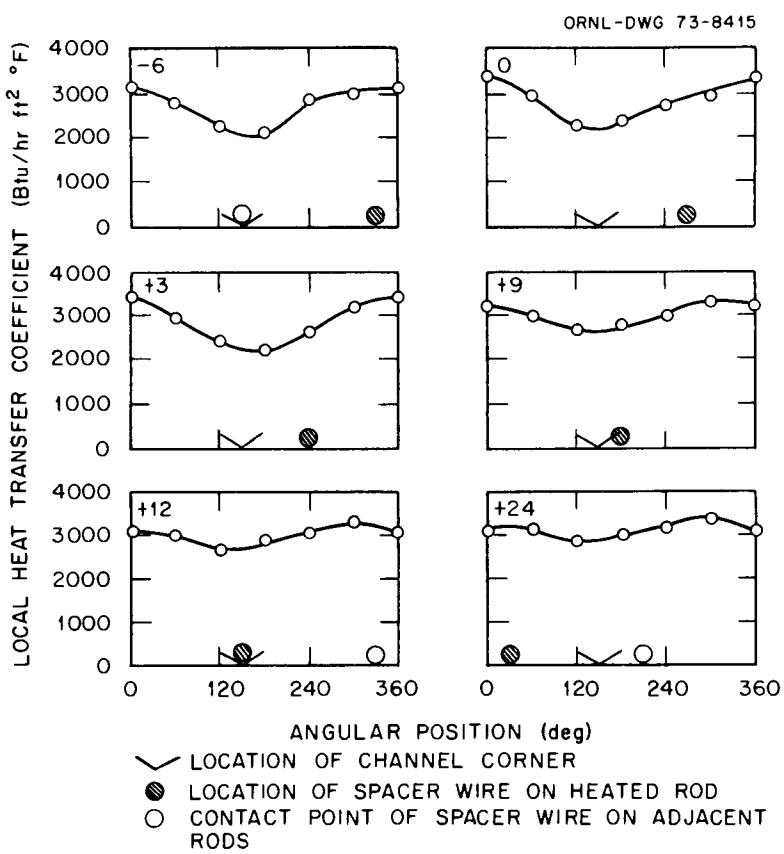

Fig. 3.1. Variation of local heat transfer coefficient in unblocked reference bundle (N_{Re} = 2.6 × 10^4; V = 10.3 fps).

when it is in place. Also shown in the figure are the locations of the channel corner and the spacer wires. Near the inlet the channel corner exerts a major influence on the circumferential variation of the heat transfer coefficient. However, near the bundle exit the circumferential variation in heat transfer coefficient becomes much smaller.

The circumferential variation in heat transfer coefficient in the presence of a heated-zone edge blockage plate is illustrated in Fig. 3.2. This figure shows results of two different tests run under substantially the same conditions. In one test, temperatures were measured every 60° as usual, while in the other test temperatures were measured every 15°. Except for the traverse 6 in. upstream of the blockage plate, the agreement is quite satisfactory; furthermore, it is clear that in most cases a true picture of the circumferential variation is obtained from readings

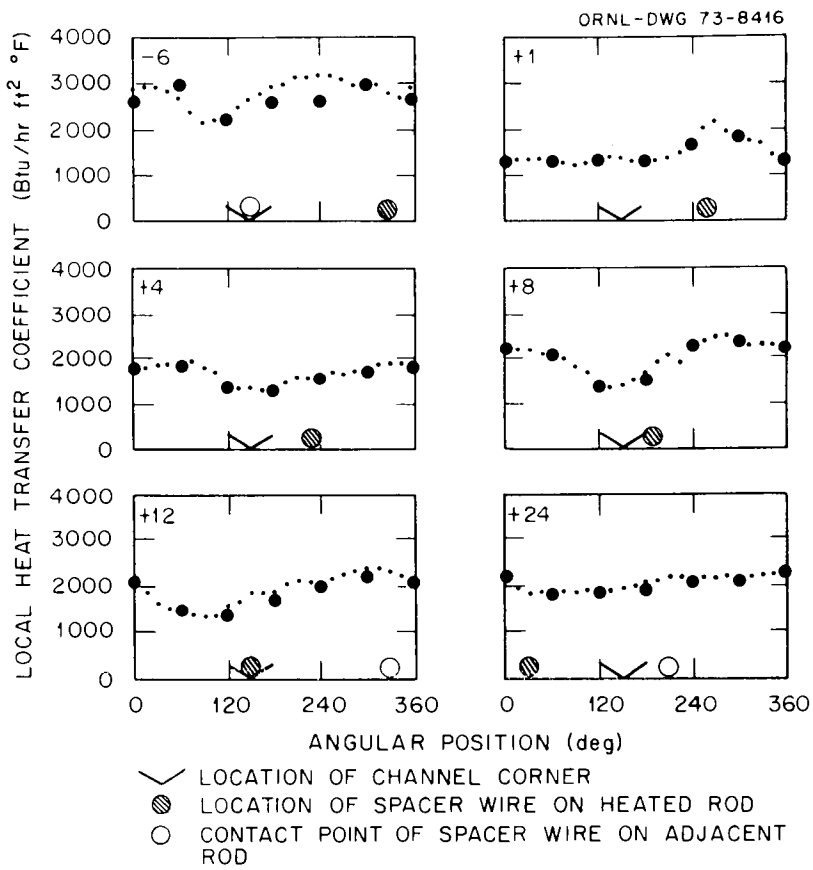

Fig. 3.2. Variation of local heat transfer coefficient in the presence of a heated-zone edge blockage plate (N_{Re} = 2.6 × 10^4; V = 10 fps).

made every 60°. As was the case in the unblocked reference bundle measurements (Fig. 3.1), the channel corner seemed to exert the greatest influence on the local heat transfer coefficient, and except for the traverse made 1 in. downstream of the blockage plate the circumferential variations for the two cases were rather similar. At a position 1 in. downstream of the blockage plate, the channel corner had little influence on the heat transfer coefficient, while the spacer wire had a noticeable effect.

The axial variation in heat transfer coefficient for these two tests (58-D and 59, Fig. 3.2) is shown in Fig. 3.3. Again, the agreement of the results for the two tests is quite satisfactory, and the flow patterns and temperature profiles are similar to those reported in the March–April bimonthly.[7]

---

7. *LMFBR Safety and Core Systems Programs Progress Report for March–April 1973*, ORNL-TM-4261.

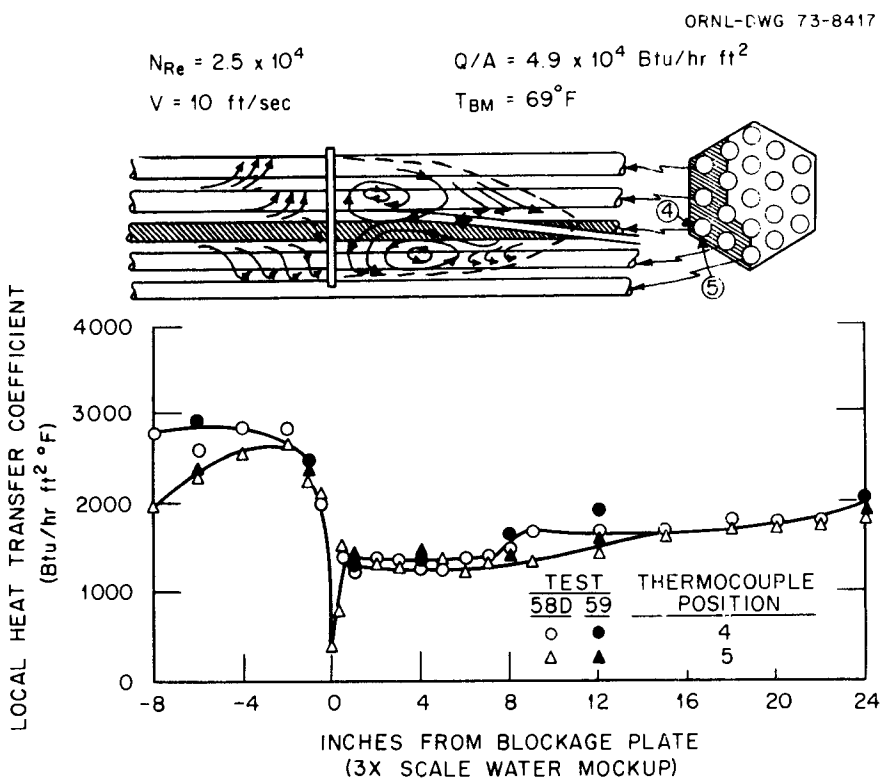

Fig. 3.3. Local heat transfer coefficients and flow patterns with an edge blockage plate in the water mockup.

Figure 3.4 shows axial variations of heat transfer coefficient and flow patterns in the vicinity of a blockage plate at the highest flow rate achieved in the edge blockage tests ($V = 28.1$ fps and $N_{Re} = 9.40 \times 10^4$). Recirculating flow regions and a strong countercurrent flow were observed in this test as in the tests at lower velocities. The end of the near-wake region is clearly identifiable by the substantial increase in heat transfer coefficient. As previously pointed out,[7] the most pronounced feature of the local heat transfer measurements is the substantial decrease in the coefficient downstream of the plate (h_1 and h_{24} are the heat transfer coefficients measured 1 in. and 24 in. downstream of the blockage plate respectively) to the heat transfer coefficient 8 in. upstream from the plate (h_{-8}):

N_{Re}	Velocity (fps)	h_1/h_{-8}	h_{24}/h_{-8}
1.14×10^4	4.66	0.50	0.64
3.04×10^4	10.0	0.42	0.72
3.95×10^4	20.0	0.34	0.68
9.40×10^4	28.1	0.30	0.65

As velocity increases, the effect of the blockage plate on the heat transfer coefficient within 1 in. of the blockage plate is markedly increased; however, at 24 in. downstream from the blockage plate, the heat transfer coefficient had recovered to 64 to 72% of the original value with no clear-cut trend with velocity.

Planar average heat transfer coefficients for the tests with an edge blockage plate are summarized in Fig. 3.5 for Reynolds numbers from 1.1 to 9.4×10^4. This figure again illustrates the marked decrease in heat transfer coefficient in the vicinity of the blockage plate (the near-wake region) and the slow recovery of the heat transfer coefficient in the far-wake region.

At the end of test 60, a slight leak developed between the blockage plate and the channel wall ∿1 1/2 tube diameters from the center line of the heated corner tube. For test 62, this leak was deliberately enlarged by forcing the plate away from the channel wall with a machine screw. Although the "silastic" sealer compound had pulled loose from the blockage

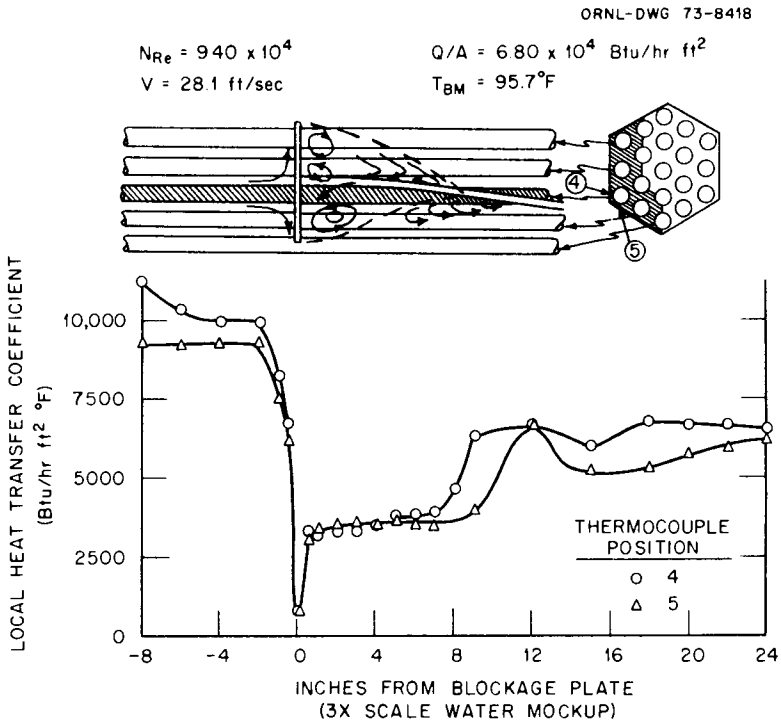

Fig. 3.4. Local heat transfer coefficients and flow patterns with an edge blockage plate in the water mockup.

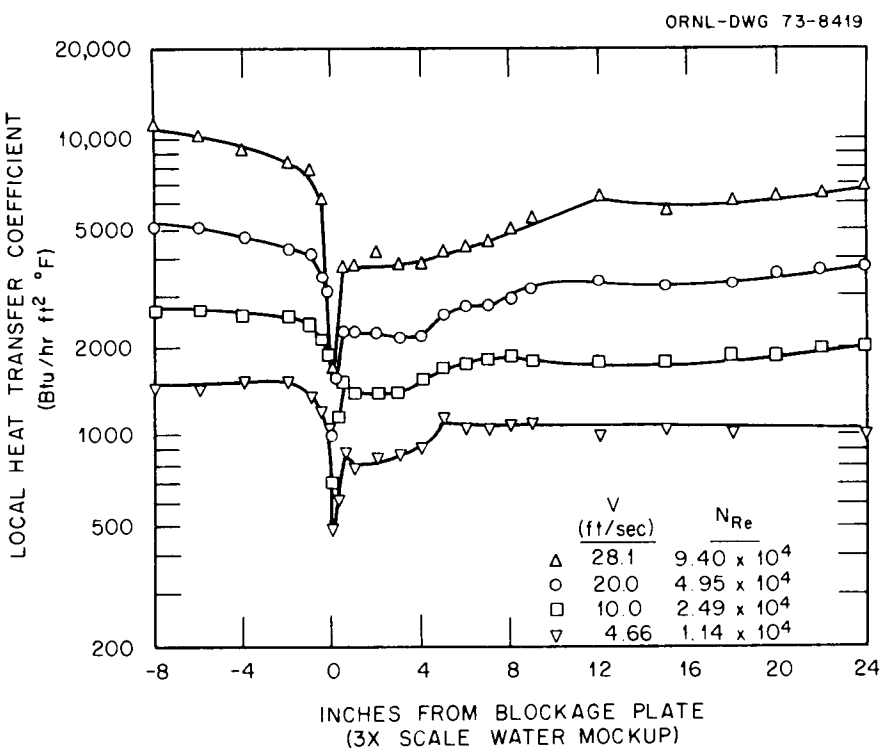

Fig. 3.5. Planar average heat transfer coefficients with an edge blockage plate in the water mockup.

plate for this test, it still remained fixed to the plate on the side toward the heated tube, so that the jet was diverted away from the heated tube. Flow visualization studies (Fig. 3.6) clearly showed the jet, but apparently it was not strong enough to completely destroy the eddy regions or the countercurrent flow observed in previous tests with no leaks. In general, two different trends were observed for the variation of heat transfer coefficient with distance from the blockage plate. These trends are illustrated in Fig. 3.7 along with results from a no-leak test (test 58-D) at the same Reynolds number for comparison. Subchannels 1, 2, and 6 all showed a pronounced peak in the heat transfer coefficient directly beneath the blockage plate. Since a machine screw was used in test 62 to hold the blockage plate away from the channel wall, it is believed that

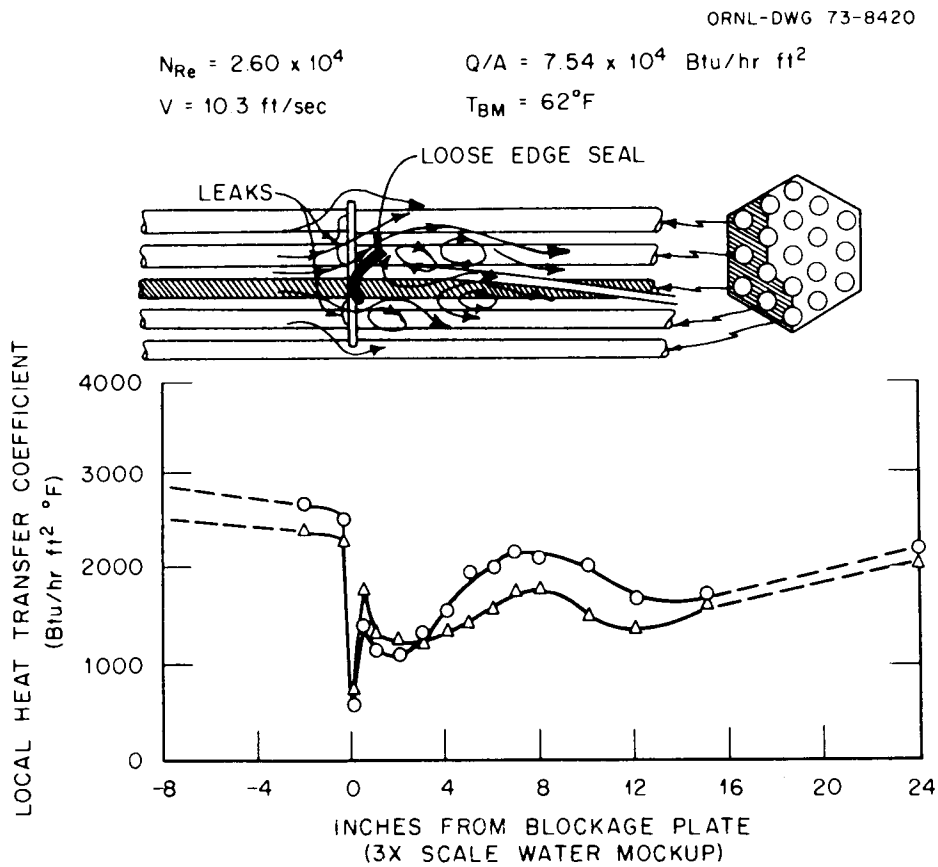

Fig. 3.6. Effect of a leak between an edge blockage plate and the channel wall on heat transfer coefficients and flow patterns in the water mockup.

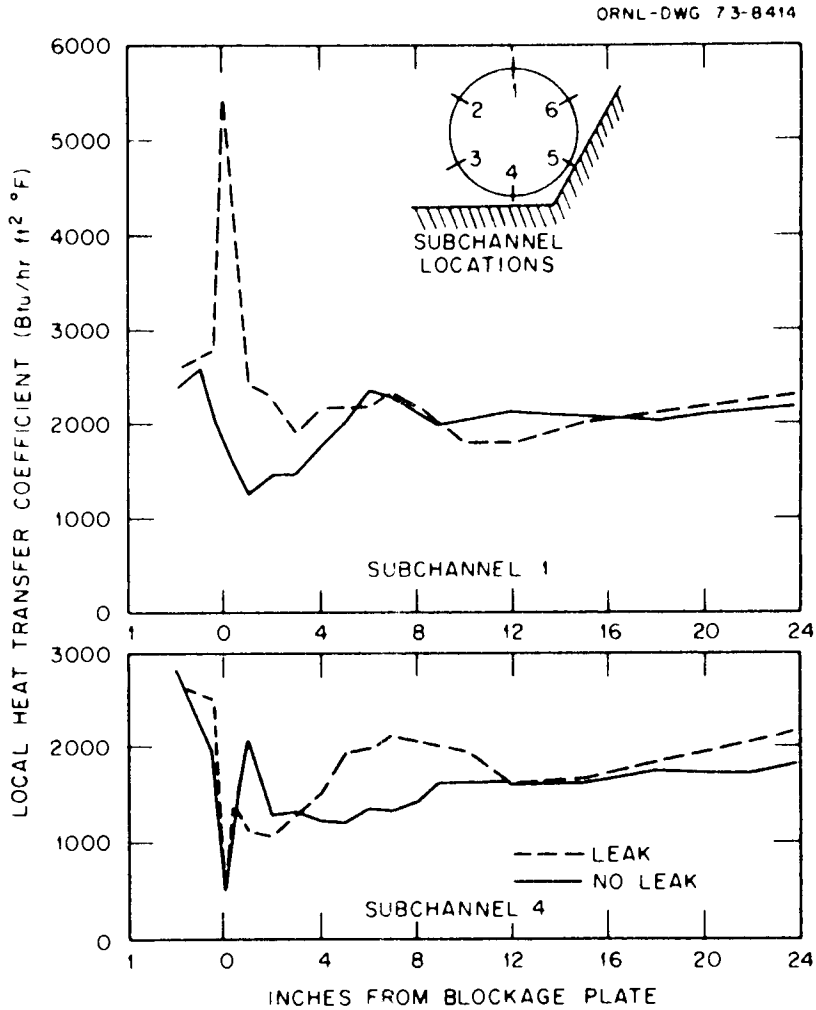

Fig. 3.7. Effect of a leak between the channel wall and an edge blockage plate on the local heat transfer coefficient.

the screw also forced the blockage plate away from the heated tube at subchannels 1, 2, and 6. However, the heat transfer coefficient for subchannels 3, 4, and 5 showed a substantial increase about 6 to 8 in. downstream of the blockage plate which is believed to be due to the primary leak between the channel wall and the blockage plate. It is notable that from about 12 in. downstream of the blockage plate, there is little evidence for any effect of the leak on the heat transfer coefficient.

As yet there are insufficient data to assess, even in a preliminary fashion, the effect of the near-wake region behind a blockage plate on

the liquid-metal heat transfer coefficients. In order to further elucidate phenomena occurring in the near-wake region, tests have been initiated in which a pulse of salt solution is injected into the near-wake region downstream of the edge blockage plate. The decay of the salt solution is then followed with conductivity probes. Preliminary analyses of the first results indicate that $35 < \tau U/d < 45$, where τ is the mean life of salt tracer in the bubble, U is the velocity approaching the blockage plate, and d is twice the largest dimension (normal to the channel wall) of the blockage plate. Further analysis is required to relate these results to temperature rise in the region downstream of a blockage plate in the liquid-metal systems.

---

4. FFM DYNAMIC TESTING AND NOISE ANALYSIS

D. N. Fry W. H. Sides

Temperature-noise monitoring at the outlet of the fuel bundle is being investigated as a means for detecting coolant channel blockage. During this reporting period bundle 3A outlet rake thermocouple signals were recorded in analog form on magnetic tape to allow off-line analysis using a digital frequency analysis program developed for the Reactor Controls Department hybrid computer. By means of this program, the analog tape-recorded signals were converted to digital signals and then processed with a fast Fourier transform algorithm to obtain the temperature-noise frequency spectra.

The bundle 3A measurements were made to accomplish three objectives: (1) to compare outlet sodium temperature noise for a blocked bundle (3A has a six-channel blockage at the 15-in. level) with previous results from an unblocked bundle (2A); (2) to determine the dependence of outlet temperature noise to changes in heater power and test section flow rate; and (3) to determine background temperature noise for the same flow conditions (but at $\sim$1/3 heater power) currently proposed for a simulated flow coastdown experiment (test 6 of test series IV).

Preliminary analysis of the recorded signals indicates that there are sufficient sodium temperature fluctuations at the rake thermocouple location to provide signals at least an order of magnitude higher than the electrical interference noise introduced by the signal conditioning amplifiers and tape recorder. Figure 4.1 illustrates a typical temperature-noise spectrum obtained from the rake thermocouple located at the

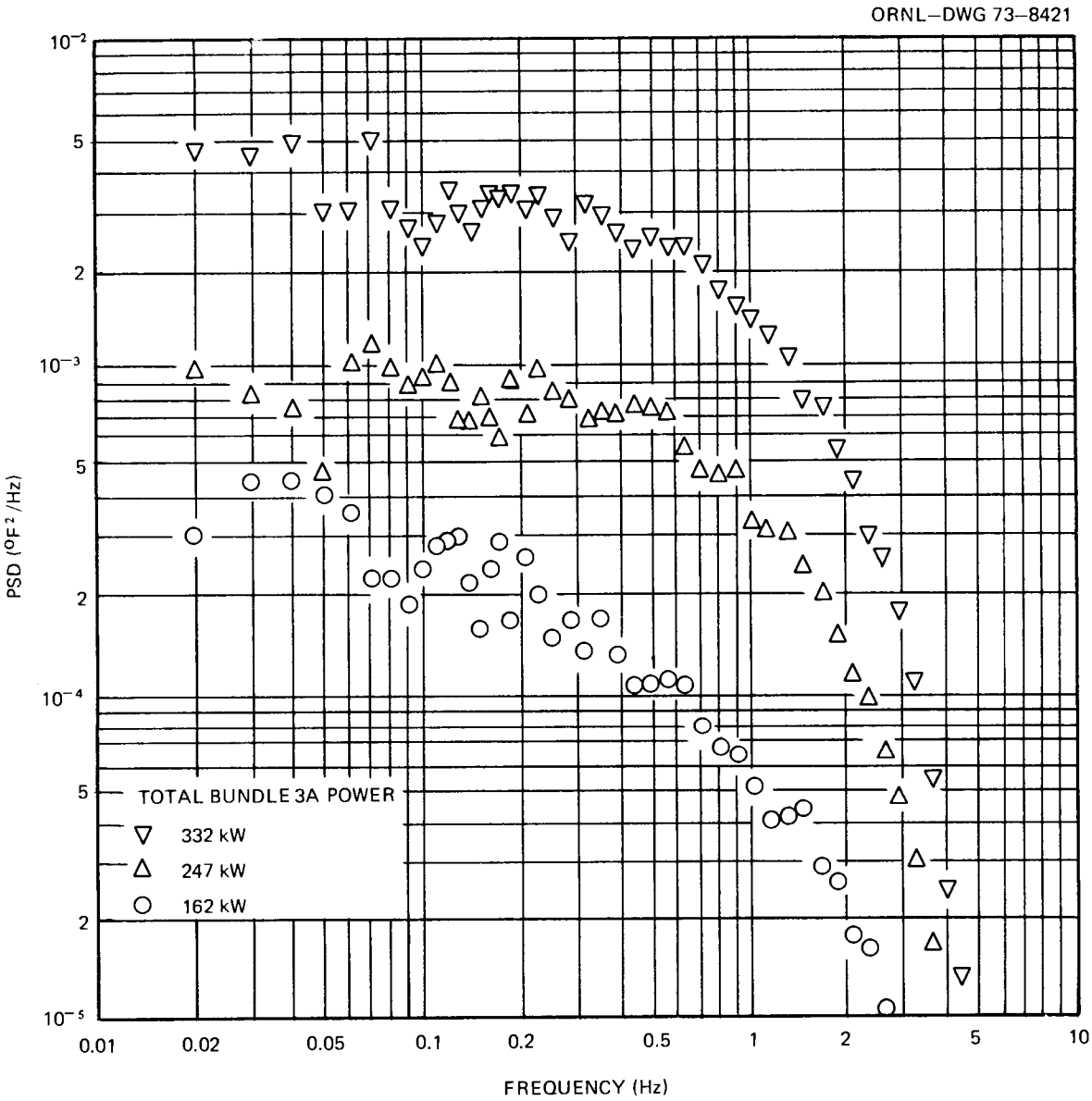

Fig. 4.1. Frequency spectra of sodium temperature fluctuations at the outlet of channel 6 for a 54-gpm flow rate.

outlet of flow channel 6 near the center of the bundle. The rolloff of the spectrum beyond ∿1 Hz is consistent with the expected time response of the rake thermocouple (a 1/16-in.-OD Chromel-Alumel insulated-junction type). As would be expected, the temperature noise increases in amplitude as the heater power is increased.

These preliminary results indicate that the three objectives stated above can be accomplished by further analysis of the signals recorded during bundle 3A operation. Final results will be reported at a later date.

---

5. FFM FACILITY ACTIVITIES

R. E. MacPherson P. A. Gnadt
L. F. Parsly

Test Bundle Operation

Bundle 1B

Information on the design and test program for bundle 1B was presented in Refs. 8 and 9, and status of the reassembly of the bundle after replacement of the failed heaters was described in Ref. 10. No work has been done on this bundle since the January–February report period. Work to reassemble the bundle to operational status will be started soon after the assembly of bundle 5A is completed. This bundle will be kept in standby in the event it is needed for fill-in testing during the operation of bundle 5A or prior to the completion of bundle 4A.

---

8. *Progress Report on LMFBR Safety Programs for September–October 1972*, ORNL-TM-4075, pp. 20–35.

9. *Progress Report on LMFBR Safety Programs for November–December 1972*, ORNL-TM-4088, pp. 27–34.

10. *LMFBR Safety and Core Systems Programs Progress Report for January–February 1973*, ORNL-TM-4148, pp. 51–55.

Test series IV (bundle 3A) test operation

Bundle 3A is designed to investigate the effects on bundle temperature of a six-channel blockage located in the heated zone of a 19-rod bundle, 15 in. downstream from the start of the heated zone. Information on the test program and initial sodium test operation of bundle 3A is presented in Refs. 11 and 12 respectively. Additional sodium testing performed during this report period is described here.

Test 4, Table 5.1, was run to determine the mixing effects in a simulated segment of an FTR fuel assembly when heating the centrally located seven heater pins with the six channels surrounding the central rod blocked.

Test 5, Table 5.2, was run to investigate whether the spiraling of the thermal streak, which was noted previously in the hexagonal duct configuration of bundle 2A and to a lesser extent in the infinite array of bundle 1B, exists in a bundle that represents an infinite array and has wire wraps installed on the dummy rods. Each of the six sets of three heaters which form the hexagonal sides of the bundle was heated separately to permit an analysis of the resulting temperature distribution. These data will be compared with appropriate data obtained with bundles 2A and 1B.

Test 6 has been redefined, as shown in Table 5.3. The object of the test will be to approach, but not produce, boiling around the center rod. The test program, which will be started early in the next report period, is designed to map the temperature effects in the bundle with respect to three variables: power, test section inlet temperature, and test section flow. The mixed-mean outlet temperature will be limited at all times to the design temperature of 1300°F; however, the center channel temperatures and heater sheaths will exceed this temperature.

We are studying design concepts of an attemperator to be placed at the test section outlet to permit operating the bundle at temperatures above 1300°F, the containment design temperature. This attemperator would

---

11. Ibid., pp. 38–51.

12. *LMFBR Safety and Core Systems Programs Progress Report for March–April 1973*, ORNL-TM-4261.

Table 5.1. Test series IV (bundle 3A), test 4

Purpose: To determine mixing effects in a simulated segment of an FTR fuel assembly when heating the centrally located seven heater pins with the six channels surrounding the central rod blocked

To compare with results from unblocked bundles

Control:

Run	Test section					
	Flow (gpm)	Inlet temperature (°F)	Outlet temperature (°F)	Power		Rod
				kW/ft	kW/rod	
101	54	600	---	10	17.5	1–7

Measure: Test section outlet temperature, °F
Heater internal temperatures, °F
Spacer wire temperatures, °F

Table 5.2. Test series IV (bundle 3A), test 5

Purpose: To investigate the extent of spiraling of the thermal streak caused by edge-row effects

To compare results with those obtained in an unblocked bundle

Control:

Run	Test section					
	Flow (gpm)	Inlet temperature (°F)	Outlet temperature (°F)	Power		Rod
				kW/ft	kW/rod	
101	54	600	---	10	17.5	16, 17, 18
102	54	600	---	10	17.5	8, 18, 19
103	54	600	---	10	17.5	8, 9, 10
104	54	600	---	10	17.5	10, 11, 12
105	54	600	---	10	17.5	12, 13, 14
106	54	600	---	10	17.5	14, 15, 16

Measure: Test section outlet temperature, °F
Spacer wire temperatures, °F
Internal heater temperatures, °F

Table 5.3. Test series IV (bundle 3A), test 6

Purpose: To simulate the effects of flow coastdown on the temperatures in the bundle with six central channels blocked in the heated zone

Control:

Run	Test section						
	Flow[a] (gpm)	Inlet temperature (°F)	Predicted ΔT	Predicted outlet temperature (°F)	Power		Rod
					kW/ft	kW/rod	
101	11.8	600	350	950	5	8.75	All
102	8.9	600	525	1125	5	8.75	
103	5.9	600	700	1300	5	8.75	
104	17.4	800	250	1050	5	8.75	
105	13.1	800	375	1175	5	8.75	
106	8.7	800	500	1300	5	8.75	
107	30.4	1000	150	1150	5	8.75	
108	22.8	1000	225	1225	5	8.75	
109	15.2	1000	300	1300	5	8.75	
110	17.8	600	350	950	7.5	11.25	
111	13.4	600	525	1125	7.5	11.25	
112	8.9	600	700	1300	7.5	11.25	
113	26.2	800	250	1050	7.5	11.25	
114	19.7	800	375	1175	7.5	11.25	
115	13.1	800	500	1300	7.5	11.25	
116	45.4	1000	150	1150	7.5	11.25	
117	34.0	1000	225	1225	7.5	11.25	
118	22.7	1000	300	1300	7.5	11.25	
119	34.8	800	250	1050	10.0	17.5	
120	26.1	800	375	1175	10.0	17.5	
121	17.4	800	500	1300	10.0	17.5	
122	60.8	1000	150	1150	10.0	17.5	
123	45.6	1000	225	1225	10.0	17.5	
124	30.4	1000	300	1300	10.0	17.5	

Measure: Test section inlet pressure, psig
Test section outlet pressure, psig
Spacer wire temperature, °F
Heater internal temperature, °F
Test section outlet temperature, °F

Special instructions:

1. The object of this test is to approach, but not produce, boiling around the center rod. The results of each run will be checked carefully and a decision reached on whether to do the next run as specified.
2. The LMFBR-data-acquisition system equipment shall be available for all tests. The high-speed scan mode of operation may be required for certain tests.
3. Acoustic monitoring equipment shall be connected during the initial runs. An evaluation will be made as to the requirement for acoustic monitoring during all phases of the test.
4. The heater winding temperature must not exceed 2200°F. Since there is a ΔT of ∿80°F/kW/ft, any local sodium temperatures (as measured by the wire-wrap thermocouples) are limited as follows (mixed-mean outlet temperatures must not exceed 1300°F):

Power (kW/ft)	Sodium temperature (°F)
5.0	1800
7.5	1600
10.0	1400

[a]Metered at sodium inlet temperature.

mix a supply stream of cool sodium taken from the bundle inlet supply with the hot sodium leaving the exit of the test bundle. If this concept proves feasible, an approach to boiling in bundle 3A should be practical without subjecting the primary pressure containment to excessive temperatures.

Status of Design and Construction of Test Bundles

Bundle 5A

Bundle 5A has been designed and built in support of the ANL FEFP P-1 experiment[13-15] to obtain information on the thermal-hydraulic characteristics of a simulated fuel bundle (19 rods). The test objectives of bundle 5A are (1) to establish operating conditions for the FEFP P-1 bundle that will produce local coolant boiling in the downstream wake of a blockage plate without significant perturbation to an overenriched fuel pin and (2) to verify optimum locations for the FEFP P-1 instrumentation and test measurements in order to relate the in-pile test measurements to the actual thermal-hydraulic coolant behavior in the FEFP P-1 bundle. ANL has recognized that the blockage may cause compatibility problems with other FEFP P-1 test objectives, and the investigation of these matters is also a part of the test objectives for bundle 5A.

A schematic cross section of the bundle which indicates the configuration and location of the blockage plate and the test bundle instrumentation is presented in Fig. 5.1. Figure 5.2 is a schematic diagram of the FFM facility and the primary facility instrumentation.

The assembly of the bundle has been completed. Figures 5.3 and 5.4 are photographs of the external and internal surfaces, respectively, of the bundle clamps. Figure 5.5 is a photograph of the assembly of the two clamps, the interior of which defines the bundle flow passage (duct). The clamps are machined to provide a "0" tolerance clearance between the

---

13. *Progress Report on LMFBR Safety Programs for November–December 1972*, ORNL-TM-4088, pp. 44–46.

14. D. H. Thompson et al., *Test Requirements for Fuel Element Failure Propagation In-Reactor Experiment P-1*, ANL/RAS 72-9, Rev. 1.

15. *LMFBR Safety and Core Systems Programs Progress Report for March–April 1973*, ORNL-TM-4261.

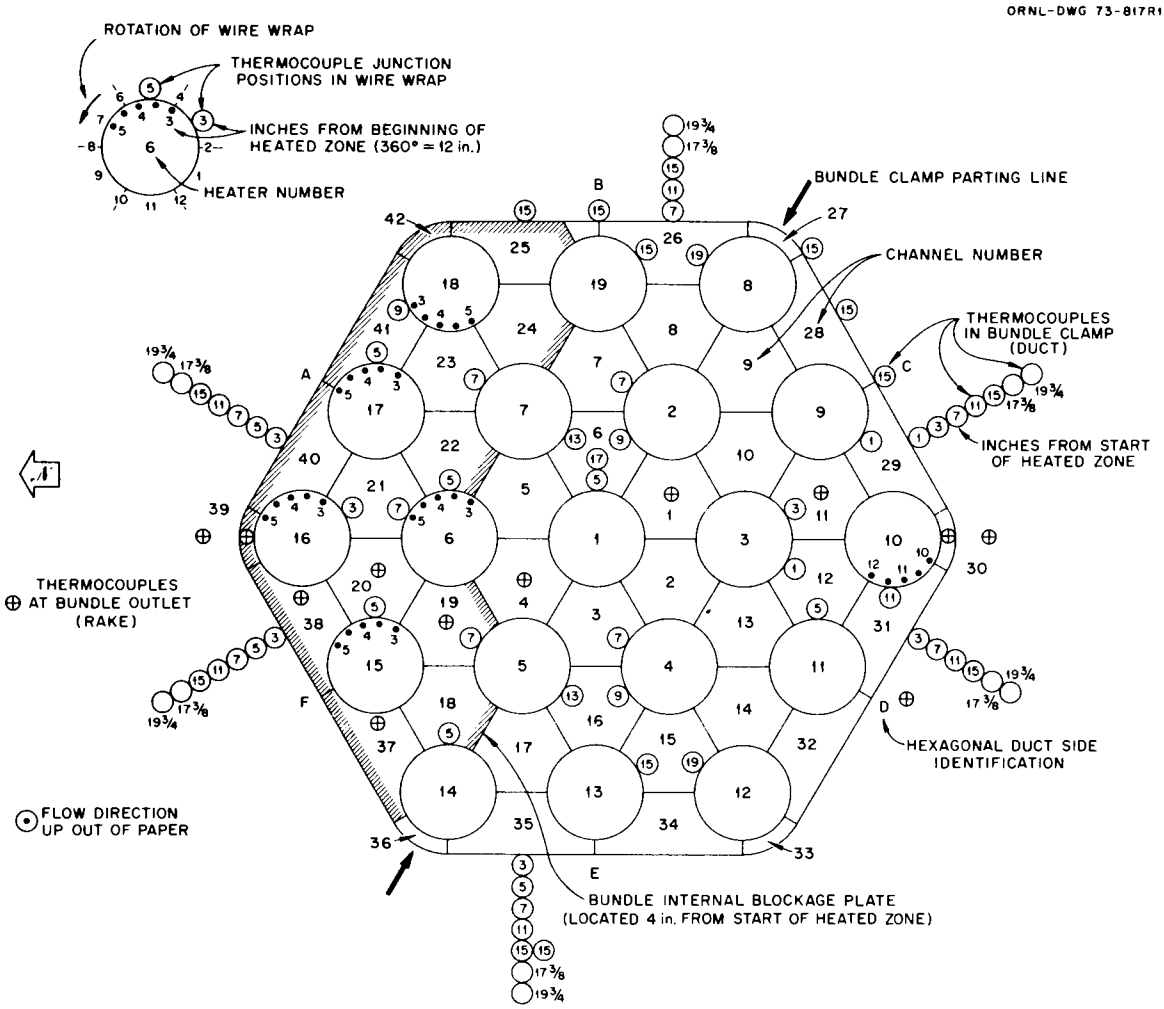

Fig. 5.1. Cross section of LMFBR-FFM bundle 5A, showing configuration of blockage and thermocouple locations in wire wraps, flow duct, and bundle outlet rake, and thermoelements on interior of heaters.

flow passage surface and the spacer wires on the outside row of bundle heaters.

Figures 5.6 and 5.7 are photographs of the blockage plate partially assembled into the bundle before the outside row of heaters are installed. Figures 5.8 and 5.9 are photographs of the bundle assembly after the blockage plate was welded in place and hand-fitted to the bundle duct surfaces. Also shown in the figures are the 0.028-in.-diam wire-wrap spacers which separate the outside row of heaters from the duct surfaces and the 0.055-in.-OD sleeves which are installed onto the 0.028-in. spacer wires to separate each heater in the outside row from adjacent heaters. The

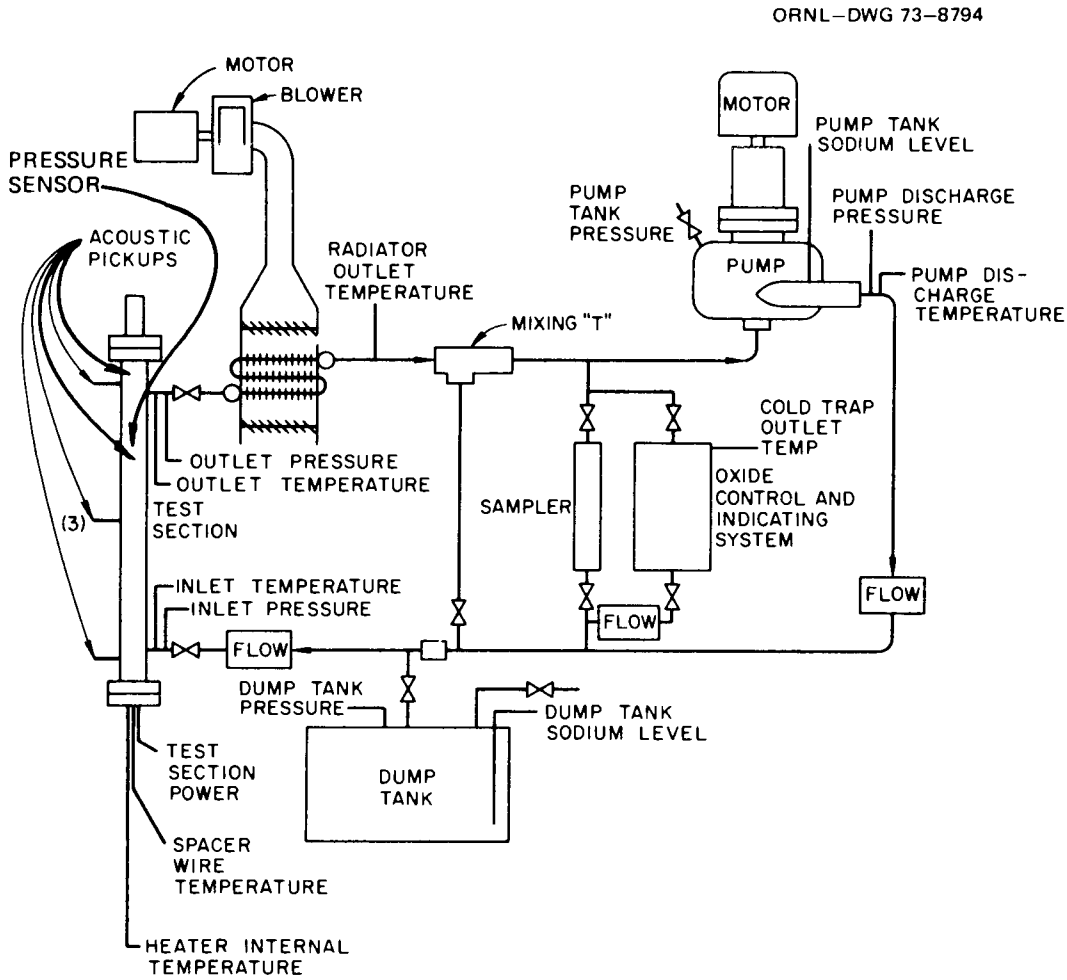

Fig. 5.2. LMFBR-FFM facility instrumentation for bundle 5A.

ends of the special adjustment screws that are to be used to hold the blockage plate against the duct wall or to space it away from the duct are also visible.

Figure 5.10 is a cross section of an elevation view of the test bundle installed into the test section housing, showing the locations of hydrophones, special acoustic sensors, and fast-response pressure transmitters, which will be tested for the first time in a sodium test facility. These sensors and pressure transmitters were furnished by ANL and are the ones presently envisioned for the FEFP P-1 test. Figure 5.11 is a cross-sectional view of the test bundle proper and shows in greater detail the blockage plate, adjustment screws, tube sheet, and thermocouple routing.

Fig. 5.3. LMFBR-FFM bundle 5A, showing exterior surfaces of two halves of bundle clamp.

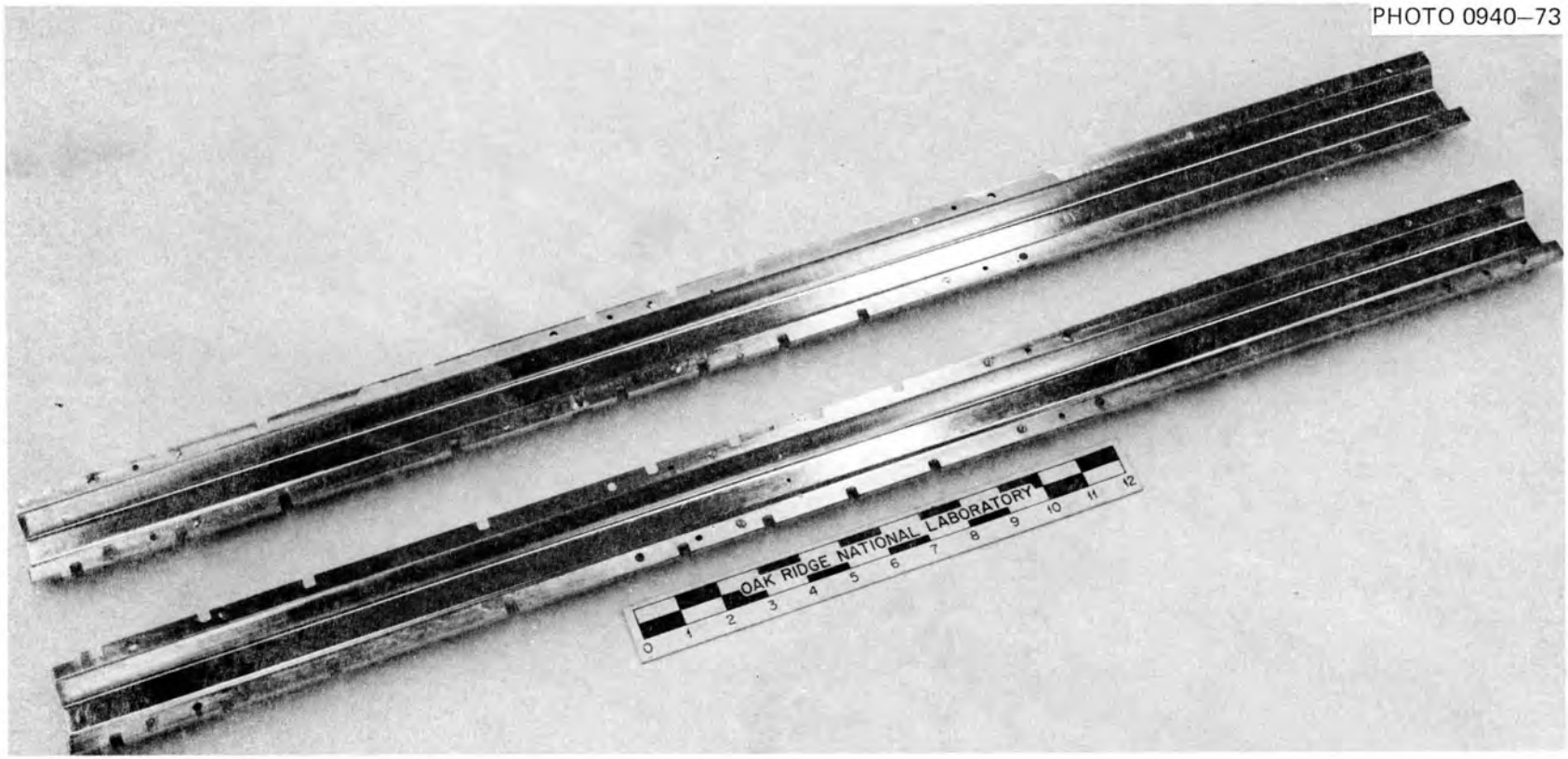

Fig. 5.4. LMFBR-FFM bundle 5A, showing interior surfaces of two halves of bundle clamp. These surfaces form the flow passage (duct) for the test bundle.

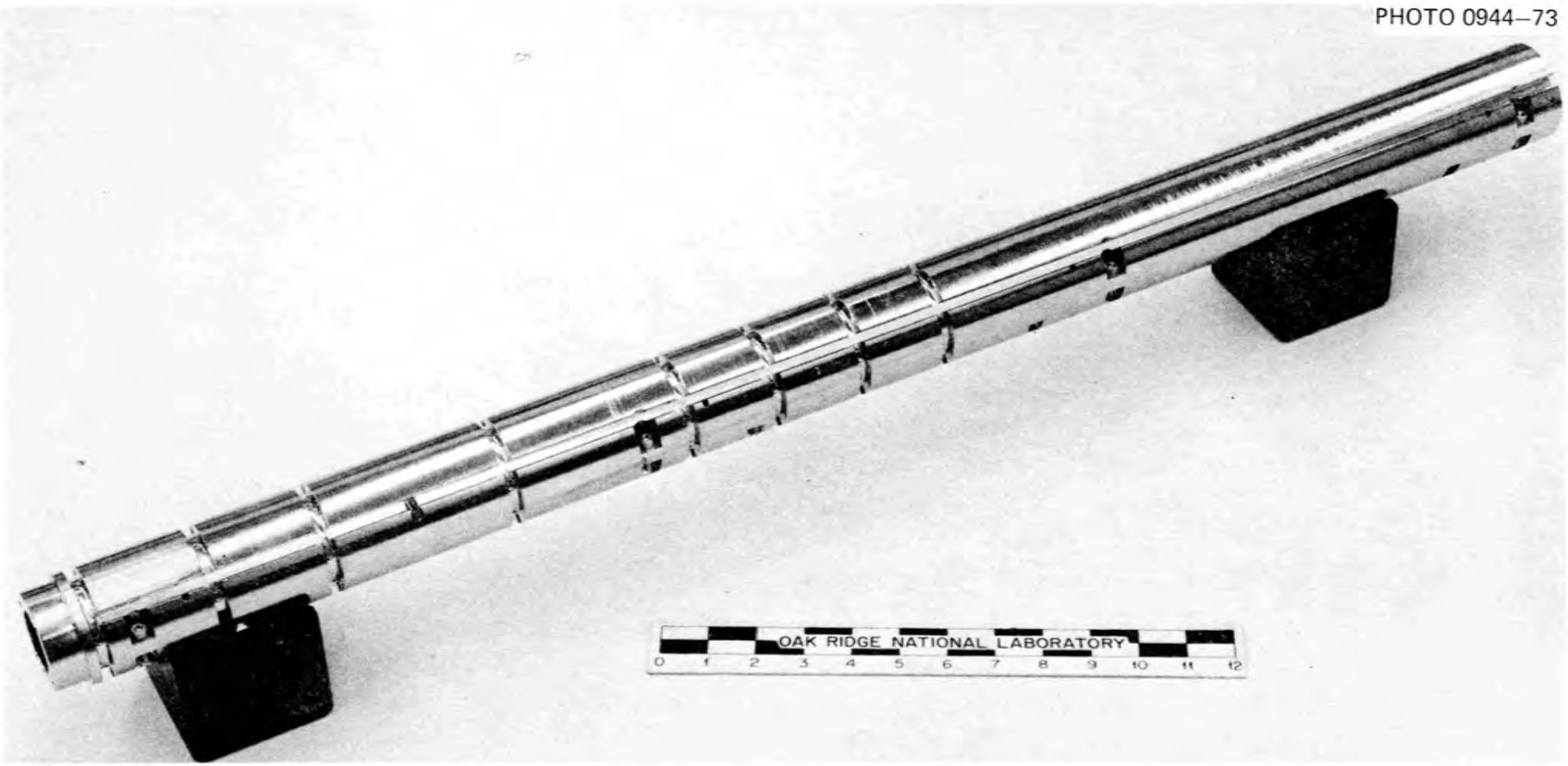

Fig. 5.5. LMFBR-FFM bundle 5A, showing two halves of bundle clamp assembled to form the flow passage (duct) for the test bundle.

Fig. 5.6. LMFBR-FFM bundle 5A, showing one view of partial assembly of the blockage plate and test bundle heaters.

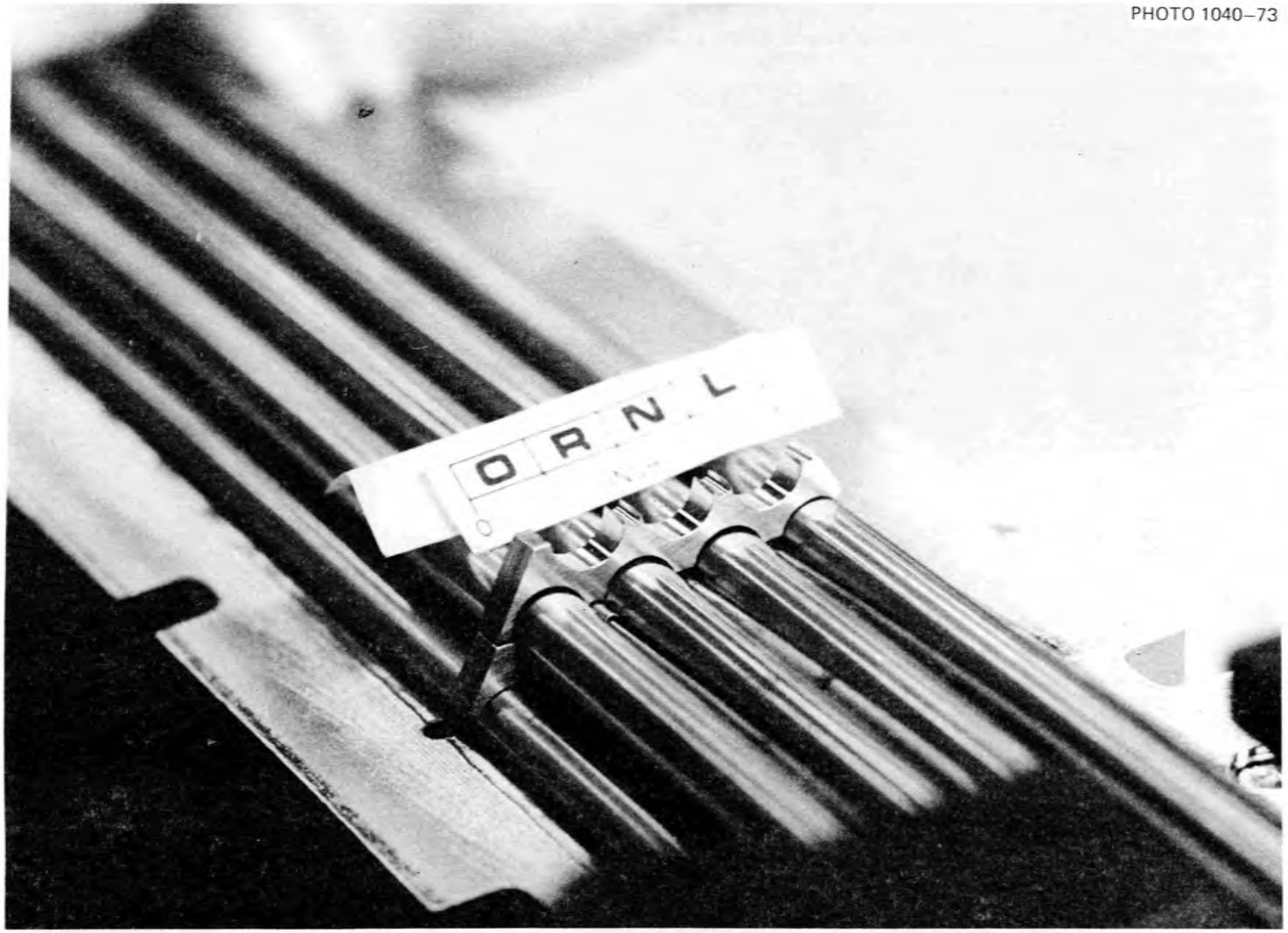

Fig. 5.7. LMFBR-FFM bundle 5A, showing second view of partial assembly of the blockage plate and test bundle heaters.

Fig. 5.8. LMFBR-FFM bundle 5A, showing the assembled blockage plate and test bundle heaters.

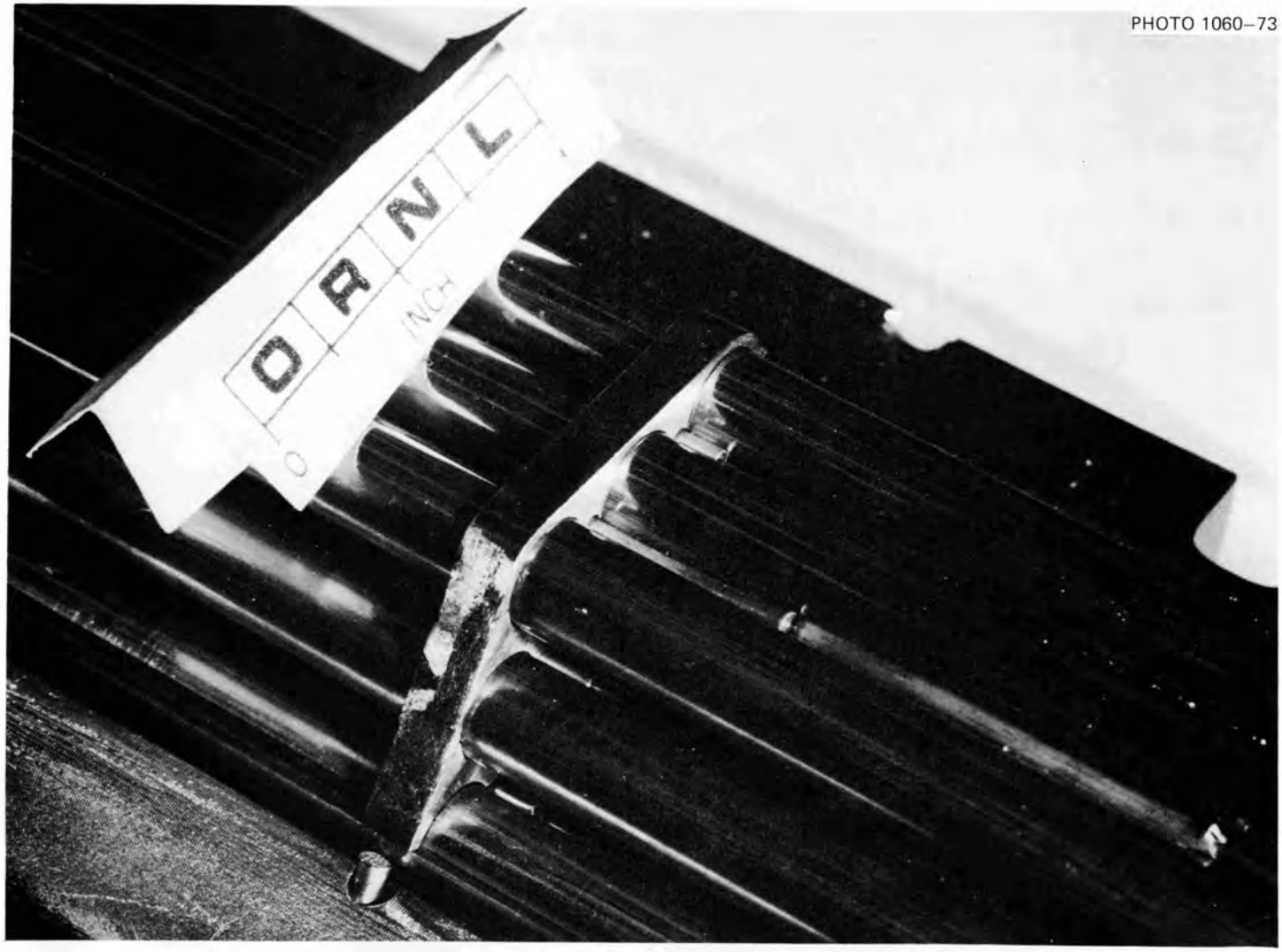

Fig. 5.9. LMFBR-FFM bundle 5A, showing second view of assembled blockage plate and test bundle heaters. Note sleeves assembled onto smaller wire-wrap spacers. Sleeves are 0.055 in. in diameter and wire-wrap spacers are 0.028 in. in diameter.

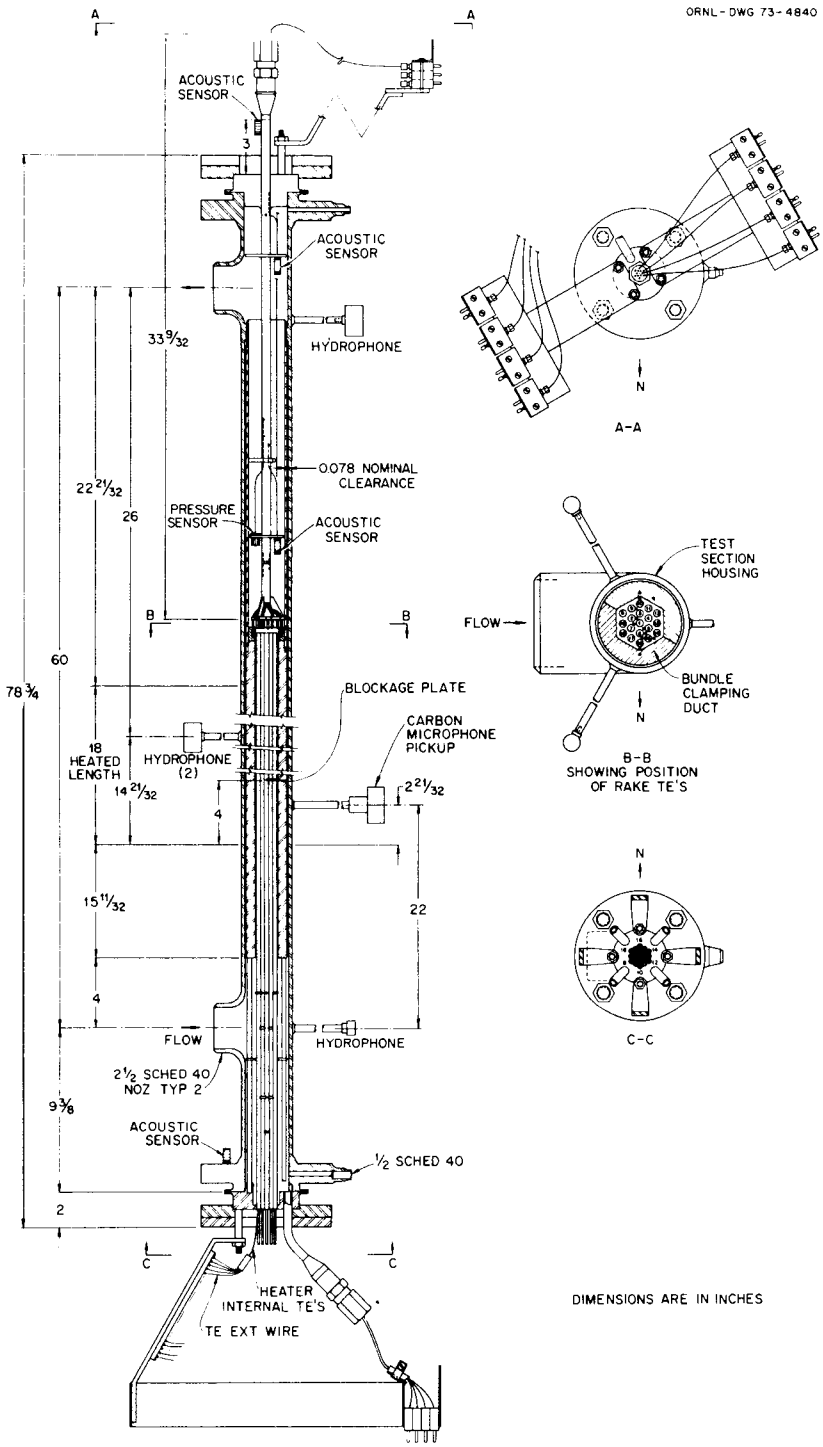

Fig. 5.10. Cross section of LMFBR-FFM bundle 5A, showing elevation view of complete test section with bundle installed. Gives elevations of blockage plate, interior acoustic pressure sensors, and exterior hydrophones and carbon microphone pickup.

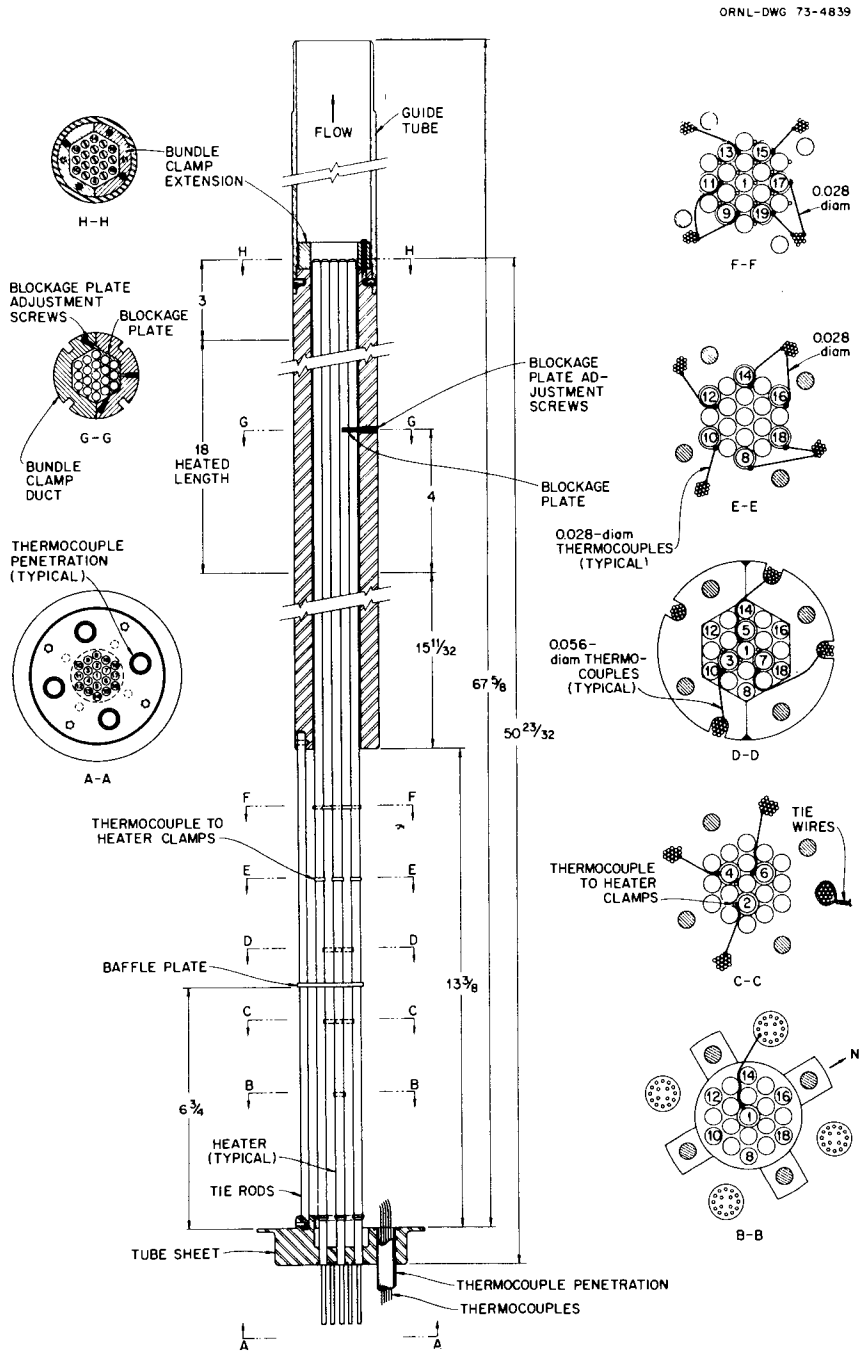

Fig. 5.11. Cross section of LMFBR-FFM bundle 5A, showing cross section of the test bundle only and elevation and plan location of blockage plate.

Test program

The test program for bundle 5A, which has been prepared, specifies eight separate test sequences, the objectives of which are briefly described below.

Test 1 will be conducted (1) to measure the pressure loss across the test section as a function of flow rate at 600°F with the blockage in position against the hexagonal duct, and (2) to obtain a calibration of the various test piece thermocouple readings as a function of flow rate.

Test 2 will be performed (1) to determine the temperature profiles typical of the FEFP in-pile loop test section with one overenriched fuel pin; (2) to determine the temperature profile behind a heated-zone blockage of the geometry to be installed in the FEFP in-pile loop test section with the blockage in position against the hexagonal duct; and (3) to determine temperatures in the hexagonal duct with one overenriched fuel pin.

Following test 2 the test bundle will be removed from the facility, and an adjustment will be made to displace the blockage plate away from the hexagonal duct and to hold it in this position.

Test 3 will be run with the main objective of determining the effect of displacing the blockage from the hexagonal duct on the temperature downstream of the blockage.

Test 4 is to determine pressure drop across the test bundle with the blockage plate displaced from the hexagonal duct and compare it with the information obtained in test 1.

Following test 4, the test bundle will be removed from the facility and the blockage plate will be removed. The bundle will then be reinstalled in the facility.

Test 5 will measure the pressure loss across the test section as a function of flow rate at a sodium temperature of 600°F with the blockage plate removed and provide base-line data for comparison with results obtained in test 1.

Test 6 will be conducted (1) to determine the temperature profiles typical of the FEFP in-pile loop test section with one overenriched fuel pin at a sodium inlet temperature of 600°F with the blockage plate removed; (2) to determine temperatures in the hexagonal duct with one overenriched fuel pin at a sodium inlet temperature of 600°F with the blockage

plate removed; and (3) to obtain base-line information to be used in evaluating the data obtained in test 2.

Following test 6, the test bundle will be removed from the facility and a new blockage plate installed. The bundle will then be reinstalled in the facility.

Test 7 will be run (1) to determine the temperature profiles typical of the FEFP in-pile loop test section with one overenriched fuel pin and will be run at a 1000°F sodium inlet temperature; (2) to determine the temperature profile behind a heated-zone blockage of the geometry to be installed in the FEFP in-pile loop test section with the blockage in position against the hexagonal duct, the same test as No. 2 except the inlet sodium temperature is 1000°F; and (3) to determine the temperatures in the hexagonal duct with one overenriched fuel pin with a 1000°F sodium inlet temperature.

After the completion of test 7, if the bundle is still viable, a decision will be reached as to the necessity of obtaining data with a 1000°F sodium inlet temperature and the blockage plate displaced away from the hexagonal can. If it is possible and seems desirable to obtain the data under these conditions, the test bundle will be removed from the facility and the blockage plate displaced the same amount as in test 3. Tests similar to those in test 3 will then be run as test 8.

Special tests

Heater bowing. Analysis of temperature data from bundle 2A operation indicated that anomalous results might be explained by heater bowing[16] (in the form of a cork screw) toward the side of the bundle which was not separated from the duct wall by the wire wraps. The evaluation by image-enhancement techniques[17] of radiographs taken of the bundle during the course of the experimental program confirmed that the bundle did bow in the manner suspected. Bundle 5A has been designed with two indexing holes for radiographic beam alignment. These holes are drilled into the bundle

---

16. *ORNL Nuclear Safety Research and Development Program Bimonthly Report for July–August 1972*, ORNL-TM-3973, pp. 3–7.

17. Ibid., pp. 37–48.

clamp (duct) 13 in. from the start of the heated zone. At this point the 0.028-in.-diam spacer wires directly separate the heaters from one duct face and are absent from the space between the heaters and the opposite duct face. By aligning the two indexing holes on the radiographic film, it should be possible to make absolute measurements of these two spaces. Radiographs of the bundle will be taken (1) at room temperature immediately after installation in the test section housing, (2) after the bundle has been preheated to 600°F and prior to filling with sodium, (3) after sodium flow has been established at 41 gpm and 600°F inlet temperature, and (4) at both 5- and 12-kW/ft heating rates on all heaters with the blockage plate against the hexagonal duct face and with the plate spaced away from the duct face.

Boiling detection. In addition to monitoring temperatures in the test bundle, several probes have been installed on the test section housing. Hydrophones have been installed in holders attached to the probes and will be monitored in an effort to establish a method of detecting boiling before supercritical boiling occurs. Two noise monitors have also been installed downstream of the test section in the sodium channel. These acoustic devices will also be monitored for indications of boiling. A fast-response pressure transmitter has also been installed in the sodium downstream from the test section. This device will be monitored for indications of high-frequency pressure pulses in an effort to determine the magnitude of local pressure perturbations during boiling. The locations of all these devices are shown in Fig. 5.10.

Bundle 4A

The detail design of bundle 4A[18,19] has progressed to a point where advanced material procurement is possible. The design of fixtures required for locating wire-wrap thermocouple junctions and for installing the wire wraps on the heaters is essentially ready for release to fabrication. Electrical design to modify the existing bundle power supply

---

18. *Progress Report on LMFBR Safety Programs for November–December 1972*, ORNL-TM-4088, pp. 36–43.

19. *LMFBR Safety and Core Systems Programs Progress Report for March–April 1973*, ORNL-TM-4261.

system is in progress. The power system modifications will provide the capability to supply thirty-seven 3-ft-long heaters at a rating of 17 kW/ft; the total power supply will be rated at 1.88 MW.

Figure 5.12 shows a facility concept which will permit continued testing of 19-pin bundles while a new addition having the larger test section housing and associated sodium components and piping for testing 37-pin bundles is being constructed.

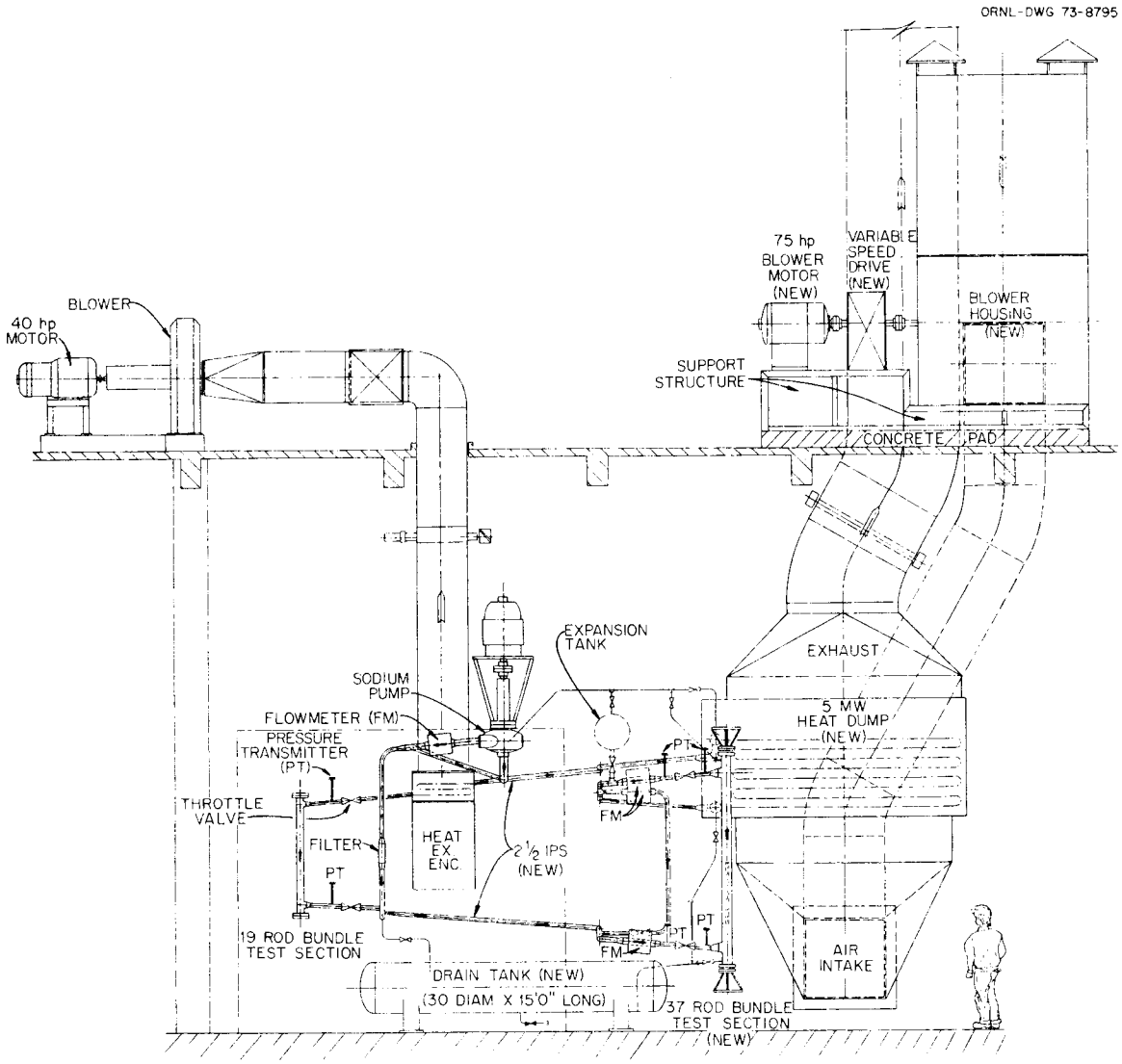

Fig. 5.12. Proposed modification to LMFBR-FFM facility. Existing 19-heater test section shown on left side. Proposed construction to accommodate 37-heater bundles shown on right side includes new drain tank, new heat sink system, new test section, and sodium piping connecting to existing sodium pump.

By locating the new addition contiguous to the east end of the present facility, the installation, testing, and inspection of most of the sodium components and piping and the installation of the associated trace heating and thermal insulation can be completed before joining the two facilities.

Flow Impedance Test

J. McCown, HEDL

At the request of RRD, a special test was conducted to investigate a possible increase in pressure drop across the bundle during steady-state, isothermal operation at 1100°F.

General

Prior to the week of May 21, 1973, the FFM loop at ORNL had operated about 1900 hr with the 19-pin bundle designated 3A. About 100 hr of this was at power (bundle heaters on). Most of the test was conducted with the loop at 600°F and a maximum of 200 to 400°F rise across the test section.

On the morning of May 21, 1973, the loop was at 650°F with an added heater on the air dump section being utilized to maintain isothermal conditions throughout. The cold trap (CT) was on line and had been held at 230 to 250°F for at least three days prior to the start of the special test.

A plugging run was made, and no plug was obtained until the plugging valve reached 210 to 215°F. The magnitude of the plug at this point indicated sodium freezing, and it was concluded the loop had less than 2.5 ppm oxygen and less than 0.15 ppm hydrogen in the sodium. The loop was then heated to 920°F, where it was held overnight.

On May 22, the temperature ascension was resumed, and 1000°F was reached by 9:00 a.m. with flows of 54 to 55 gpm in the section. A plugging run was made, and three small breaks were obtained (0.02–0.04 gpm), with the highest occurring at about 550°F. By 11:00 a.m., the loop was at 1100°F with the CT on line at 250°F, and a flow sweep was made over the range of 20 to 55 gpm (see Fig. 5.13). At this point, some unusual flow behavior was already noticeable in the auxiliary circuit.

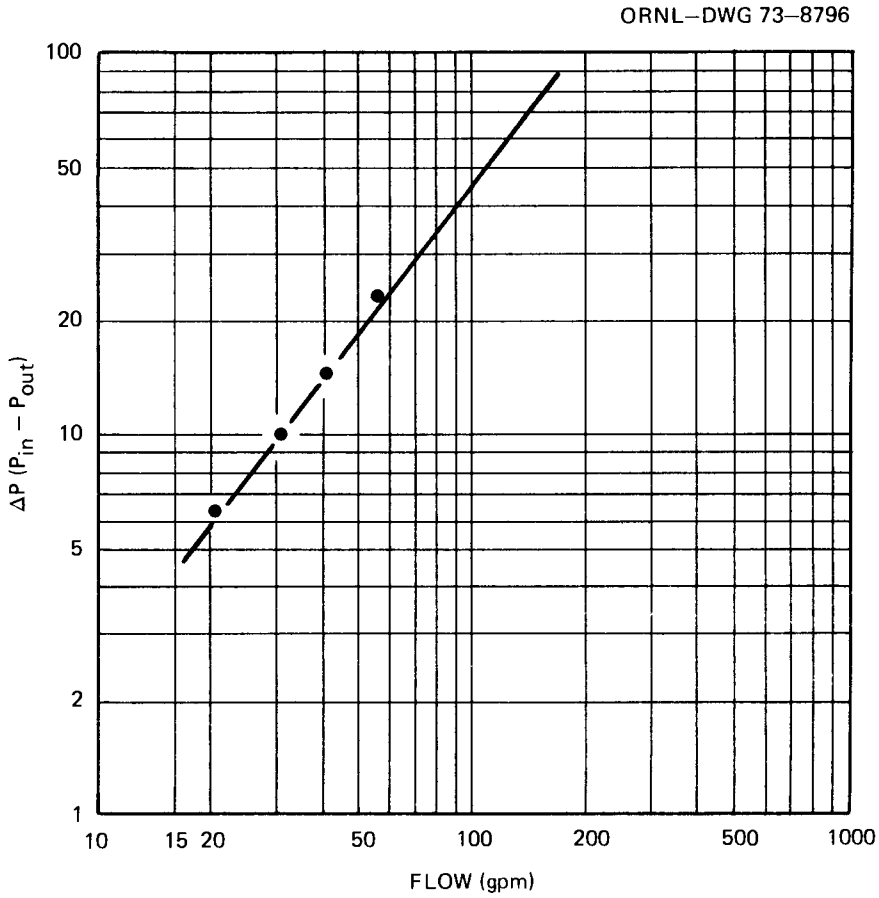

Fig. 5.13. FFM flow sweeps at 1100°F, May 22 to May 25, 1973.

A second plugging run (for the day was started at ∿1:30 p.m., and several plugs were obtained over the range of 380 to 570°F. Their rate of formation and amount of flow change were considerably greater than during the 9:30 a.m. plugging run. Holding the plugging valve at 380°F caused a continuous flow decrease which was more pronounced than that discussed later. A repeat of the 40-gpm flow sweep point was made and the loop returned to 54 to 55 gpm for the night.

On the morning of May 23, flow in the CT circuit had dropped ∿0.7 gpm. It had been necessary to increase it at 10:30 p.m. on May 22 to prevent a total loss of flow during the night. The loop was still holding 1100 ± 10°F. A plugging run was started which differed from the May 22 afternoon run, in that less high plugging material was seen and the main break was obtained at 300°F. This temperature, after correction

for supercooling, agrees well with the CT temperature of 340°F reached during the night due to the CT circuit flow decreases. The plugging meter was operated in the cyclic mode over two plug-unplug cycles at the 300°F plugging point.

A flow-through sampler tube was brought on line for 4 hr at 1100°F and shut off at 4:30 p.m. (lines were left heated in order to resume sampler flow the next morning) (see Fig. 5.14).

On the morning of May 24, it was noted that decreases in flow in the CT circuit had ceased about 6:00 p.m. on May 23 and had reversed and continued to increase during the night. This caused a rise in CT temperature to about 350°F for 1 to 2 hr. The CT temperature was reset to 250°F by 9:00 a.m. Attempts to reestablish flow in the sampler lines were unsucessful. Increased heating and valve cycling did not work, and the sampler was secured for line draining and cooldown in the afternoon.

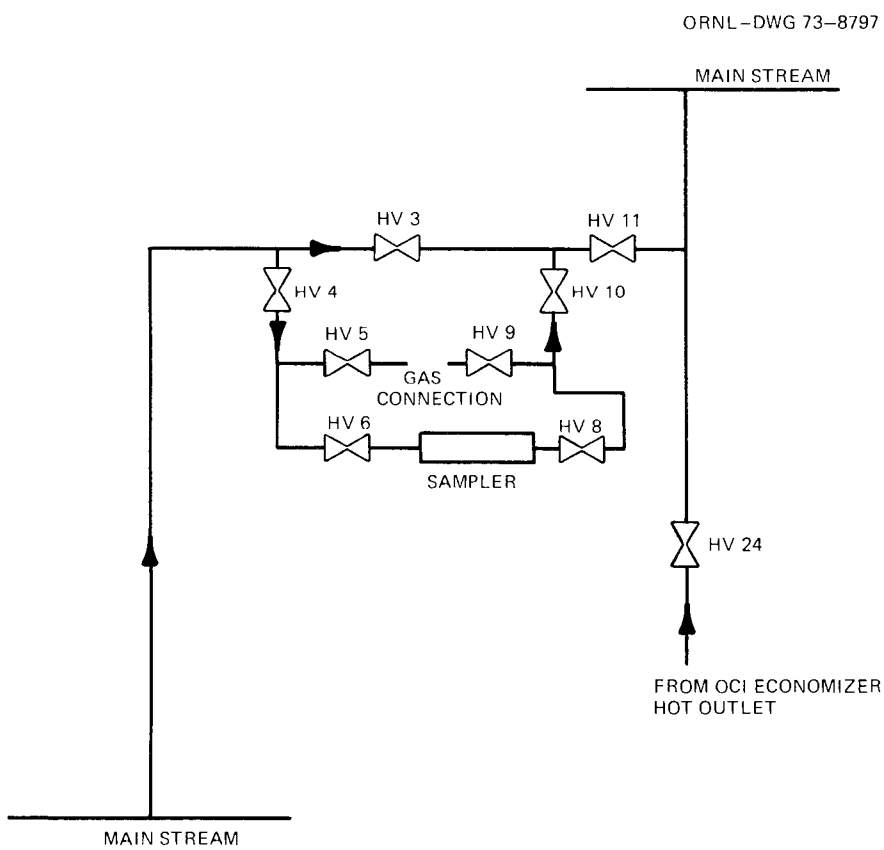

Fig. 5.14. Flow-through sampler arrangement. Sampler shut down by closing HV 6 and HV 8 and opening bypass HV 3. Temperature from 8V 4 → HV 10 was at 600°F overnight.

A plugging run was made over the range 630 to 225°F, and a break (plug) was found at 240°F, but the blower would not cool the system below 220°F.

Since the Oak Ridge area was experiencing thunderstorm activities, which threatened to scram the loop during the night, a flow sweep was made starting at 1:15 p.m. A continuous slight increase in the CT circuit flow was noted throughout the day (∿0.1 gpm/hr).

By the morning of May 25 flow in all circuits was level and normal. A final flow sweep was performed (loop still at 1100°F) and a final plugging run made. No plugs were found, and the run appeared identical to the one performed on May 21 at 650°F. The flow sweep and ΔP data taken are discussed later.

Anomalous behavior in auxiliary circuits

Cold trap. The FFM is equipped with a Mine Safety Appliances oxygen control and indicating (OCI) system. One bad feature of the system is the use of a common heat exchanger (HX) for the CT and plugging meter and the fact that the HX is several feet away from the CT crystallizer with a valve in the connecting line (see Fig. 5.15).

Shortly after reaching 1100°F, a continuous decrease in flow in the CT circuit was evident. Heating the line and valve between the HX and crystallizer to 530°F resulted in a slower rate of flow decrease but did not stop it.

Plugging meter. When the CT was shut off and the plugging meter brought on line at 600°F, sodium was going into the HX and replacing the much cooler (<350°F) sodium from the CT outlet. Each time, this resulted in a change from flow decrease to flow increase in the OCI circuit.

During early plugging runs, when flow was switched from the CT to the fluted valve circuit, the flow rate in the OCI circuit changed markedly. By the morning of May 23, this was not the case. The CT valve was opened and closed three times while the plugging valve was cycled three times, and no flow change occurred in the OCI circuit. This indicated that a plug had formed upstream from the CT valve, probably in the cold side of the economizer. Heating up the plugging valve and economizer section caused a flow increase which substantiates the plug location.

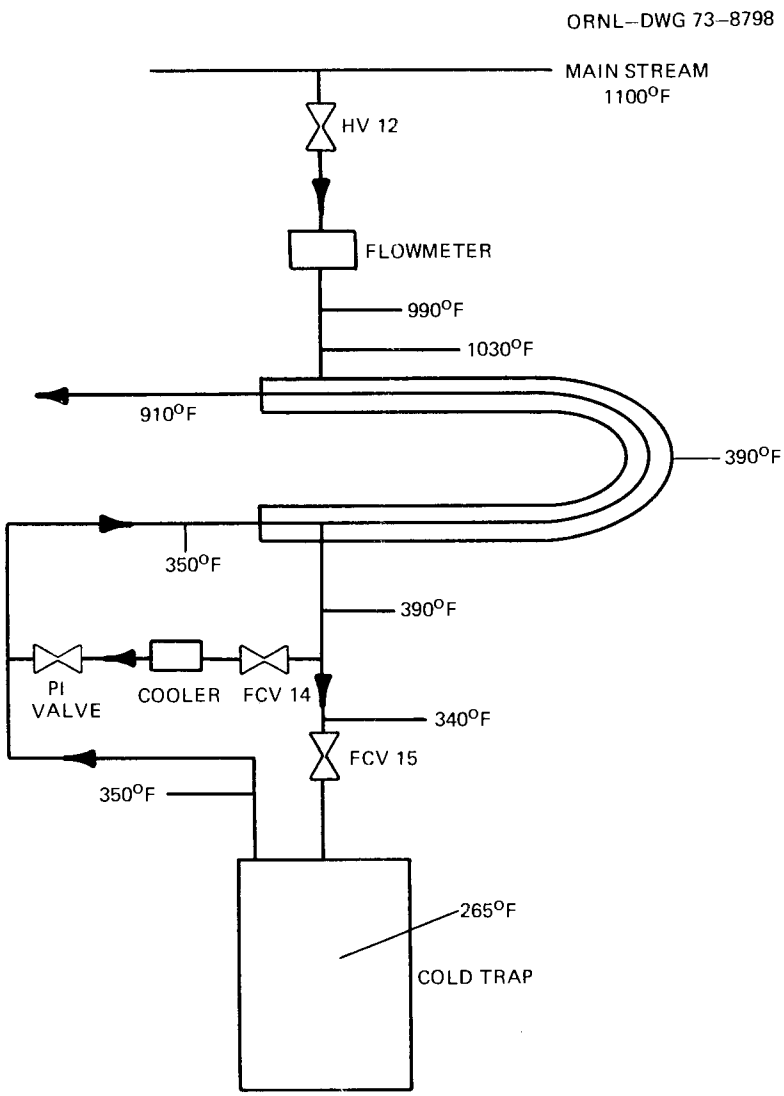

Fig. 5.15. MSA-OCI system on FFM. Temperature profile recorded during afternoon of May 22 prior to increasing heat to line and FCV 15. Continuous flow decrease in this system started the morning of May 22.

During one plugging run, the OCI economizer was not performing well (the cooler would not go down below 220°F). (This is the same behavior exhibited by the PAL PTI which we treated as economizer surface fouling.)

Auxiliary circuit flow patterns. The flow in the OCI circuit generally stays constant unless the plugging valve is cooled to the point of impurity precipitation or sodium freeze-out. During these tests, continuous flow decreases were noted for the first 30 hr at 1100°F (except as noted above). These changes were generally on the order of −0.1 gpm/hr. During the night

of May 23, this trend reversed, and continuous flow increases of about the same magnitude were noted for over 24 hr. By the final day, the flow pattern had returned to normal (steady flow — CT on line).

Sampler system. The flow-through sampler was originally brought on line by the standard ORNL procedure for heating and valve positioning. After 4 hr of flow at 1100°F, both sampler valves were closed, and bypass flow around the sampler section was resumed. The time of shutdown corresponds well with the period during which OCI flow decreases ceased and reversed direction to steady increases. The following morning, it was found impossible to reestablish flow in the sampler. The valves were cycled and lines heated up to 600 to 700°F (this is also identical to sampler problems encountered on PAL during high-temperature operations). The sampler, together with valves and line stubs, is presently en route to HEDL for examination.

Flow impedance

The main test purpose was to investigate flow impedance changes across test section inlet and outlet pressure transducers at flows of ∿25 fps (54.6 gpm). Two tests to demonstrate ΔP changes previously used on CCTL and JOYO data included a plot of ΔP vs flow rate and a plot of $\Delta P/(\text{gpm})^2$ at 1100°F and 54.6 gpm. The FFM flow sweep data are shown in Fig. 5.13. Flow impedance data are shown in Fig. 5.16 and compared with CCTL Mark IIA in Fig. 5.17.

Conclusions

The 2 to 2.5% change in flow impedance which was noted is not large enough to prove the effect was real. Slight changes in temperature and flow rate appeared to affect the data, as did flow sweep measurements. There is no doubt, however, that holding the loop above 1000°F did result in the formation of a high plugging material. This material appeared in plugging runs, in flow decreases in auxiliary circuits, in flow trend reversals with temperature changes, and in a plugged up sampler system. The correlation between these occurrences and the leveling out and decrease

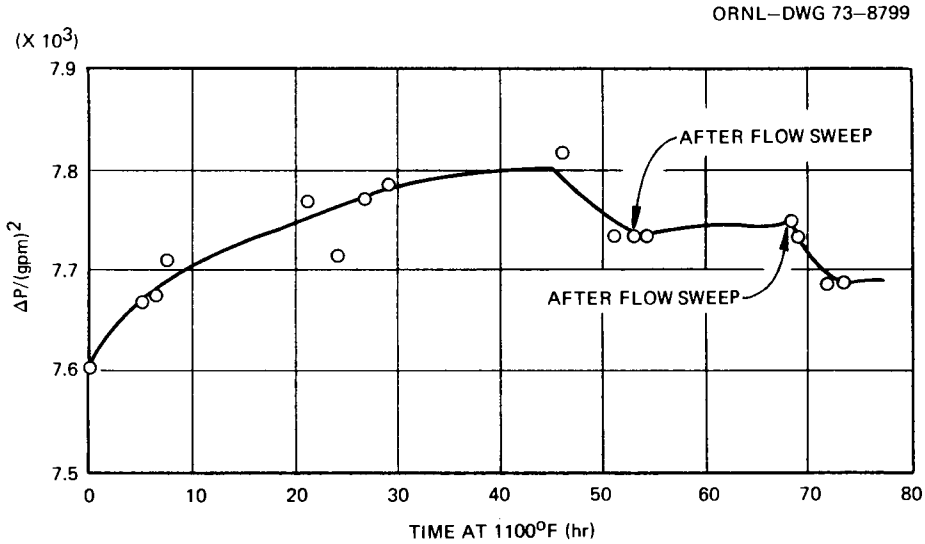

Fig. 5.16. Flow impedance change at 1100°F and 25 fps.

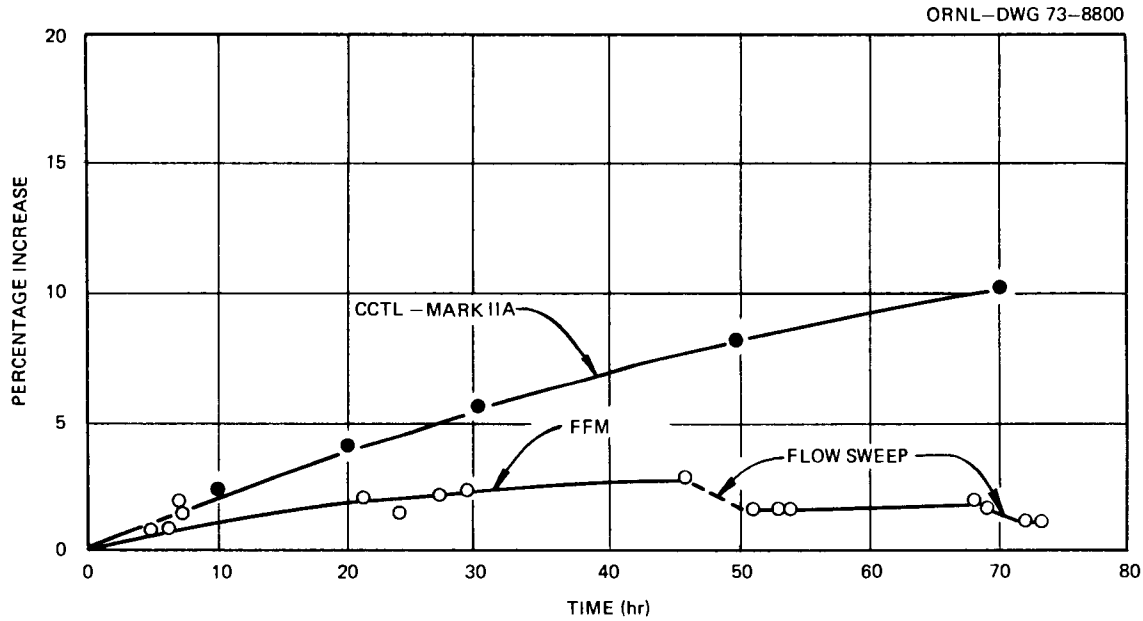

Fig. 5.17. Flow impedance change at 1100°F and 25 fps compared with CCTL Mark IIA.

in the $\Delta P/(gpm)^2$ values, strongly indicates that the flow impedance phenomenon is related to and/or caused by the formation of the high-temperature plugging species. Oxygen and hydrogen levels (as controlled by the cold trap) are not causing the behavior noted.

6. HEATER DEVELOPMENT

R. E. MacPherson D. L. Clark

The objectives of this program are to provide heaters for the FFM, to assist in the procurement of heaters for other LMFBR investigators, to develop both a category II heater that can withstand transients to the point of boiling at a heat flux of 10^6 Btu hr^{-1} ft^{-2} and a category III heater that can withstand sodium expulsion and reentry at the same heat flux, and to develop heaters for the water reactor safety program.

Miscellaneous items covered in this report period are discussed immediately below. Next, the work on the prototypic FFM heaters is discussed followed by the work on advanced heaters, including the category II and III heater development.

Revision of AEC-RDT Standard P4-1

Revision 1 of AEC-RDT Standard P4-1T, Electric Heaters — Simulated LMFBR Fuel Pins, was completed and issued for approval of June 19, 1973. Comments will be evaluated and resolved as soon as practical. Publication of the revision is tentatively scheduled for August 1973.

Heaters for the ANL OPERA Flow Blockage Test

Fabrication of these 17 heaters by Watlow was completed at the end of June 1973, and an ORNL inspector at Watlow provided the required inspection services. The first heater fabricated had a heated length of 36 1/2 in., which was slightly over the specified 36 ± 1/4 in., and allowances were made to correct this variance for the remainder of the heaters. The results of ORNL inspections will be sent to ANL during the first week in July.

Westinghouse-ARD Blanket Heaters

A meeting was held with personnel from W-ARD and Watlow to complete the specifications for blanket simulation heaters. RDT Standard P4-1 with

modifications will be used to procure the heaters. These modifications agree in general with the modifications in Rev. 1 of RDT P4-1.

Review of HEDL Specification HWS-9178

In accordance with requests from AEC-DRRD and HEDL, HEDL specification HWS-9178 was reviewed, and assistance will be given in the bid evaluation. The specification covers The 2.3 Megawatt Sodium Heater Assembly, HTR-400, for the Prototype Closed Loop Development Installation at HEDL. Comments on the specification discussed by telecon with HEDL personnel were covered in a memorandum issued by HEDL. Formal distribution of comments on the specification and bid package will be made by ORNL.

PWR Fuel Pin Simulators for the ORNL BDHT Test

Experience obtained in the work on LMFBR fuel pin simulators is being utilized to assist the PWR Blowdown Heat Transfer Separate Effects Program (BDHT) at ORNL. Investigations were made of both cartridge and direct (skin-heated) heaters.

Job specification E-10520-RM-004-S-0, Specification for Electrically Heated Tapered Wall Tubular Element, was transmitted to AEC-DRRD for comments by cover letter, BDHT-0810. However, pursuant to other decisions, this specification is now dormant, and efforts are concentrated on producing indirect heaters of the cartridge type.

ORNL received, inspected, and accepted three indirect heaters[20] from Watlow. These 20-ft-long, 0.422-in.-OD heaters have 12-ft-long heated sections and are rated at 135 kW. A stepped-chopped-cosine heat flux distribution was provided using a tubular central heating element with various sized tubular sleeves placed over the central tube in the lower heat flux sections. Twenty thermocouples are provided for each heater, eight in the interior of the heating element and the remainder in the double-walled heater sheath.

---

20. *LMFBR Safety and Core Systems Programs Progress Report for March–April 1973*, ORNL-TM-4261.

One of these heaters was installed in the Thermal-Hydraulic Test Facility (THTF) and sustained six blowdown tests during June 1973. The initial test was run at 70 kW and the other five at 150 kW. During these tests the heater was operated for a total of 36 hr, with 12 hr at 120 kW or more and 4.5 hr at 150 kW. There were 22 On-Off operations performed at elevated power levels.

Data from these tests will be analyzed in detail, but preliminary indications show no degradation of the heater, and all 20 thermocouples are still operative. The heater is scheduled for a total of ten blowdowns, after which a second heater will be tested.

FFM Heaters

This section is concerned with the design, testing, and evaluation of heaters for the FFM facility.

Heaters for FFM bundle 5A

The instrumented heaters for bundle 5A were received, given a routine anneal for straightening purposes, and delivered to the FFM project. During initial assembly activities it was decided that the heaters needed further straightening. This was accomplished by placing the heaters in the straightening fixture and reannealing for 10 min in hydrogen at 950°C (reported previously as 1000°C).[20]

After reannealing, the heaters had a slight continuous bow which was traced to the restraining action of the internal sheathed thermoelements located in a 90° quadrant on one side of the heater sheath ID. Since this bow was slight, it could be accommodated by the bundle design. In the future, consideration will be given to locating the thermoelements uniformly around the entire 360° circumference. This should also minimize heating element eccentricity effects which can be caused by locating the thermoelements within a single quadrant.

Prior to reannealing these particular heaters only, the five sheathed thermoelements had been "stored" by wrapping them around the 0.093-in.-diam copper power lead. This was done to protect the thermoelements from damage during subsequent assembly operations, particularly during the

electron beam welding of the heater sheaths to the tube sheet where the electron beam is, of necessity, very close to both the thermoelements and the copper leads. Following reannealing of the heaters and assembly of the heater bundle, attempts to make electrical connections to the Alumel thermoelements were unsuccessful because of brittleness. All the thermoelements either fell off when the sheath was removed or came loose when attempts were made to check them with a continuity meter.

A detailed investigation was conducted and an incident report written on these Alumel thermoelements. Their embrittlement has effectively eliminated the usefulness of the internal thermocouples in this particular batch of heaters. The investigation indicated that "exaggerated grain growth" occurred in the Alumel wires (approximately 0.005 in. diam) as a result of the annealing of the heater with the thermoelements coiled around (stored on) the 0.093-in.-diam copper leads. This coiling, which had not previously been done prior to annealing, resulted in approximately 5% cold work of the Alumel and Chromel wires, and the grain growth during annealing resulted essentially in a single grain structure across the Alumel wire. This grain growth occurs primarily in pure or low-alloyed material of small size where the amount of cold work is slight. Supporting studies will be supplied with the final incident report.

The loss of the internal thermocouples does not prevent the use of these heaters, and since they had been assembled into the FFM bundle 5A prior to discovery of the problem, they will be used for initial sodium tests in the FFM. Replacement instrumented heaters have been ordered for July 1973 delivery and will be installed in the bundle at an appropriate time.

The prototype instrumented heater for bundle 5A is being operated at 11 kW/ft with the sodium outlet temperature at 1200°F. Some boiling runs at 1 to 7 psia and 1200 to 1500°F sodium temperature were made with the heater to aid in the testing of boiling detection equipment. The total operational testing of 68.7 hr includes 31.5 hr at 11 kW/ft and 1200°F sodium outlet temperature. Following testing at 12 kW/ft and the same outlet temperature, the test will be stopped and investigations made to determine the cause of a continuing decrease in the heater resistance.

Heaters for FFM bundle 4A

Fabrication of the two prototypic heaters was delayed by a vendor's oversight in the procurement of the Kanthal A-1 heating element material. All materials are now in the vendor's plant, and fabrication should begin immediately. Delivery of the prototypes is expected by mid-July, with the production units scheduled for fabrication immediately after satisfactory performance of the prototypes in sodium tests.

Advanced Heater Development

This section covers the procurement and testing of category II and III heaters, evaluation of heater fabrication, and the redesign of the heater test facility.

Category II heaters

The principal features, materials, and status of the various category II heaters tested, received, or on order are shown in Table 6.1. Reference 20 discusses the status of these heaters at the end of the previous report period. The heating element material for items 1 to 5 is Nichrome V and for items 6 to 11 is Kanthal A-1, which has been selected as the category II heating element material. Item 12 is a category III heater.

Category II heaters with Kanthal A-1 heater elements

ARI, Inc., heater. The ARI heater failed after 0.9 hr operation at 16 kW/ft and a sodium outlet temperature of 1200°F. Previous operation at reduced power and lower sodium temperature conditions totaled 58 hr. This heater was accepted with a short molybdenum section because the vendor was unable to attach molybdenum to copper. Although the shortened length was not ideal, it was not judged to be the cause of the heater failure. Upon investigation it was found that the Kanthal A-1 ribbon had melted at its connection to the molybdenum lead. A similar degradation of the Kanthal A-1 was occurring at the other end of the heater in the connection of the ribbon to the molybdenum ground lead extension. This problem should be eliminated by using an alternative material that has good welding characteristics with the Kanthal A-1 ribbon.

Table 6.1. Category II and III heaters[a]

Item No.	Vendor	Annular insulating material	Mandrel insulating material	Purchase date	Comments, operating status, and analysis
1	Watlow	Union Carbide TS-945 BN	Coors vitreous aluminum oxide	10-12-71	Failed at void in alumina at 12.5 kW/ft with 1200°F Na due to reaction associated with low-thermal conductivity of machine-filled BN and void in alumina mandrel; five internal sheathed TEs
2	ARI	Union Carbide HD-0092 BN	Union Carbide HD-0092 BN rod	10-12-71	Failed at 10 kW/ft and 1000°F Na by element melting due to low and nonuniform density (and thermal conductivity) of the BN
3a	SDI	Carborundum HP heat 8153 BN powder	Union Carbide HD-0092 BN rod	10-12-71	Failed at 10 kW/ft and 1000°F Na by element melting due to low and nonuniform density (and thermal conductivity) of the BN
3b	SDI	Union Carbide HD-0092	Union Carbide HD-0092 BN rod	7-10-72	Failed at 10 kW/ft and 1000°F Na after 8 hr due to melting of last inch of heating element; average BN density of 77%, but low density in failed area
4	Watlow	Carborundum type A BN tube	Coors vitreous aluminum oxide	11-30-71	Failed at 4.8 kW/ft due to poor connection between copper lead in and heating element plus poor thermal contact with BN in this area; replacement heater is undergoing final inspection at ORNL
5	SDI	Carborundum type A BN tube	Coors vitreous aluminum oxide	11-30-71	Inspection revealed poor thermal contact between heating element and BN at junctions in BN annular tubes; unable to establish appropriate thermal contact; unit will not be tested at present
6	Watlow	Union Carbide HD-0092 BN	Union Carbide HD-0092 BN rod	∿5-1-72	Heater operated at 18 kW/ft (1,020,000 Btu hr^{-1} ft^{-2}) in 1200°F Na; failed on cycling test at same heat flux when Na flashes into boiling at ∿30 psia (saturation temperature of 1785°F)
7	SDI	Union Carbide HD-0092 BN	Union Carbide HD-0092 BN rod	∿5-1-72	Rejected due to poor and nonuniform BN density; replacement heater shipped on June 22, 1973

Table 6.1 (continued)

Item No.	Vendor	Annular insulating material	Mandrel insulating material	Purchase date	Comments, operating status, and analysis
8	RAMA	Union Carbide HD-0092 BN	Union Carbide HD-0092 BN rod	∿5-1-72	Connection between heater element and molybdenum ground lead extension failed after 36-hr operation with 0.7 hr at 14 kW/ft and sodium outlet at 1200°F; poor weld structure is suspected, and future design will be changed
9	SEMCO	Union Carbide HD-0092 BN	Union Carbide HD-0092 BN rod	∿5-1-72	Heating element melted after 35 hr testing and 2 hr at 18 kW/ft and 1200°F sodium outlet; a second unit will be ordered
10	ARI	Union Carbide HD-0092 BN	Union Carbide HD-0092 BN rod	∿5-1-72	Connections between heater element and molybdenum ground lead extension and intermediate material failed after 59 hr operation with the last 0.9 hr at 16 kW/ft and sodium outlet at 1200°F; see item 8 above also
11	Watlow	Union Carbide HD-0092 BN	Union Carbide HD-0092 BN rod	∿10-16-72	Successfully operated for 307 hr at 18 kW/ft and 1200°F sodium; 10 transients at 18 kW/ft to 1800°F sodium previously performed and 40 more scheduled in order to fill all specified category II requirements; internal thermal elements still operative
12	Watlow (category III)	Union Carbide HD-0092 BN	Union Carbide HD-0092 BN rod	∿10-16-72	Operated for 60 hr with 20.6 hr at 18 kW/ft and 1200°F followed by 12 transients leading into sodium boiling with 8 transients at 18 kW/ft and saturation temperature of 1820°F; failed by sheath melting when flash boiling occurred; additional unit(s) will be ordered

[a]Items 1 to 5 have Nichrome V heating elements; items 6 to 11 have Kanthal A-1 heating elements; and item 12 has a Pt–8% W heating element and is a category III heater. Additional prototypes have been ordered for items 8 to 12.

A second unit is on requisition in which AISI 316L stainless steel rod will be substituted for the molybdenum lead.

RAMA heater. The heater failed after 35.7 hr total operation. During the last hour of operation the test conditions were 14 kW/ft (∿800,000 Btu hr^{-1} ft^{-2}) at a sodium outlet temperature of 1200°F. The failure occurred at the junction of the Kanthal A-1 heating element to the molybdenum ground extension lead and involved melting of the Kanthal A-1 without short-circuiting to the heater sheath and was identical to the failure in the ARI heater reported above.

A second unit is on requisition in which AISI 316L stainless steel rod will be substituted for the molybdenum rod.

Watlow heater. Two "loss-of-flow" transients were run on the instrumented category II (item 11) heater obtained from Watlow before failure occurred; these are in addition to the ten transients reported previously. During the first transient at 18 kW/ft, a calculated external temperature of 1740°F was reached. During the second transient at 18 kW/ft, in which a calculated sheath external temperature of 1800°F was reached, the heater power circuit was opened (scrammed) by high current. Although investigation indicated a possible short circuit approximately two-thirds along the heating element, the short circuit cleared when low power was restored. Power was then increased to 18 kW/ft, but the heater power was scrammed as the sodium temperature increased to just above 1000°F. The test was stopped, and inspection and radiography of the heater revealed a short circuit between the heating element and the sheath approximately two-thirds along the heater element. The internal sheathed thermoelements, which are closer to the heater sheath than the heating element at the site of short circuit, were still operative. There was no sign of deterioration of the heating element along its entire length, including the site of the short circuit. These items of evidence led us to believe that the short circuit was due to a conductive inclusion in the insulation near where the arc occurred.

SDI heaters. Two category II heaters have been fabricated for item 7 and shipped by SDI. The annulus in one heater is filled with Union Carbide Corporation (UCAR) grade TS-1206 BN powder and the other with UCAR HD-0092 BN powder. Mandrels made of HD-0092 BN are used in both heaters.

Inspection and tests on both heaters will be performed as soon as practical.

Qualifying manufacturers of category II heaters

Attempts are still being made to qualify additional manufacturers to category II requirements. Replacement orders have been given to SEMCO, RAMA, and ARI, each having shown a reasonable degree of technical competence. A similar order will be placed with SDI if testing justifies it.

An order for two additional category II heaters has been placed with Watlow with TS-1206 BN powder to be used in one heater and HD-0092 BN powder to be used in the other.

Category III heaters

An order for two additional category III heaters[21] has been placed with Watlow. One heater is a modified, uninstrumented categroy III heater with a 0.150-in.-OD heating element, 12 in. long, made of Pt–8% W alloy to permit operation at heat fluxes up to 1.6×10^6 Btu hr^{-1} ft^{-2} at sodium temperatures up to 1400°F or higher.

Evaluation of heater fabrication methods

A second dummy heater,[21] in addition to the one described in the previous report, was fabricated. Although infrared scans of both heaters indicated some variation in density of compacted boron nitride, the compaction was superior to that observed in industrial heaters. However, the variation in density must be reduced further before a satisfactory standard heater can be produced. The two heaters will be sectioned for final characterization of the heating element, boron nitride insulation, and the sheath.

A meeting was held with representatives of Union Carbide Corporation in Cleveland, Ohio, to discuss the feasibility of using crushable boron nitride preforms as insulation throughout the heater. Two methods appeared to be feasible, and both will be investigated.

---

21. *LMFBR Safety and Core Systems Programs Progress Report for March–April 1973*, ORNL-TM-4261.

In one method, tubular forms of UCAR HD-0092 would be machined in the appropriate lengths by Union Carbide or others from hot-pressed material. Some machining[22] has been done previously on other hot-pressed boron nitride materials; however, these materials were used as close-fitting parts in an unswaged heater assembly. The use of machined hot-pressed preforms in a swaged heater has not yet been attempted.

In the other method, powdered HD-0092 or TS-1206 material would be cold pressed in suitable dies to the required configuration. In general, such cold pressing would be restricted to length-to-diameter ratios of 1 or less in order to prevent spalling. The cost and limited lifetime of suitable dies might eliminate this method from detailed consideration.

An additional disclosure of interest at this meeting was the previous use of HD-0092 BN forms as thermocouple insulators for a NASA development program. Further details have been requested, but the prime consideration in the development had been the high thermal conductivity of BN, which would result in a faster time response for an insulated-junction thermocouple. Of further interest would be a possible decrease in the disturbance of the thermal conductance path in which such thermocouples might be placed. Additional information on this development has been requested.

Redesign of the heater test facility

The Quality Assurance Program Plan[21] was completed and approved. Procurement of material and parts is under way, and a schedule for the fabrication and construction activities will be established in the immediate future.

---

22. *ORNL Nuclear Safety Research and Development Program Bimonthy Report for March–April 1972*, ORNL-TM-3831, p. 46.

ORNL-TM-4331
UC-79e, UC-79p

Internal Distribution

1. N. J. Ackerman
2. R. K. Adams
3. A. H. Anderson
4. S. E. Beall
5. M. Bender
6. R. H. Bryan
7. J. R. Buchanan
8. R. M. Burnett
9. C. J. Claffey
10. D. L. Clark
11. C. W. Collins
12. Wm. B. Cottrell
13. F. L. Culler, Jr.
14. W. F. Ferguson
15-19. M. H. Fontana
20. A. P. Fraas
21. D. N. Fry
22. P. A. Gnadt
23. A. G. Grindell
24. W. O. Harms
25. R. B. Heimdahl
26. H. W. Hoffman
27. S. I. Kaplan
28. P. R. Kasten
29. T. S. Kress
30. R. Kryter
31. R. N. Lyon
32. R. E. MacPherson
33. F. C. Maienschein
34. C. D. Martin
35. H. C. McCurdy
36. C. K. McGlothlan
37. A. J. Miller
38. R. L. Moore
39. F. H. Neill
40. L. C. Oakes
41. L. F. Parsly
42. P. Patriarca
43. A. M. Perry
44. M. W. Rosenthal
45. T. H. Row
46. J. P. Sanders
47. R. L. Scott
48-49. Myrtleen Sheldon
50. R. H. Sigler
51. M. J. Skinner
52. I. Spiewak
53. R. D. Stulting
54. D. A. Sundberg
55. D. G. Thomas
56. D. B. Trauger
57. W. E. Unger
58. J. L. Wantland
59. A. M. Weinberg
60. J. R. Weir
61. G. D. Whitman
62. T. Kerlin (Consultant)
63. R. Saxe (Consultant)
64. M. Leverett (Consultant)
65. W. McCarthy (Consultant)
66-67. Central Research Library
68. Y-12 Document Reference Section
69-71. Laboratory Records Department
72. Laboratory Records (RC)

External Distribution

73-74. Director, USAEC Division of Reactor Research and Development, Washington, D.C. 20545
75. Director, Division of Reactor Safety Research, USAEC, Washington, D.C. 20545
76. USAEC-RRD Senior Site Representative, Oak Ridge National Laboratory, P. O. Box X, Oak Ridge, Tennessee 37830
77. Research and Technical Support Division, USAEC Oak Ridge Operations Office, P. O. Box E, Oak Ridge, Tennessee 37830
78-336. For distribution as shown in TID-4500 under category UC-79e and UC-79p, Liquid Metal Fast Breeder Reactors (Safety and Reactor Core Systems)

☆U.S. GOVERNMENT PRINTING OFFICE: 1973-747-302/43